HSE and Re-Os systematics of the 3.3 Ga Weltevreden komatiites from the Barberton Greenstone Belt, South Africa: Implications for early Earth's mantle evolution

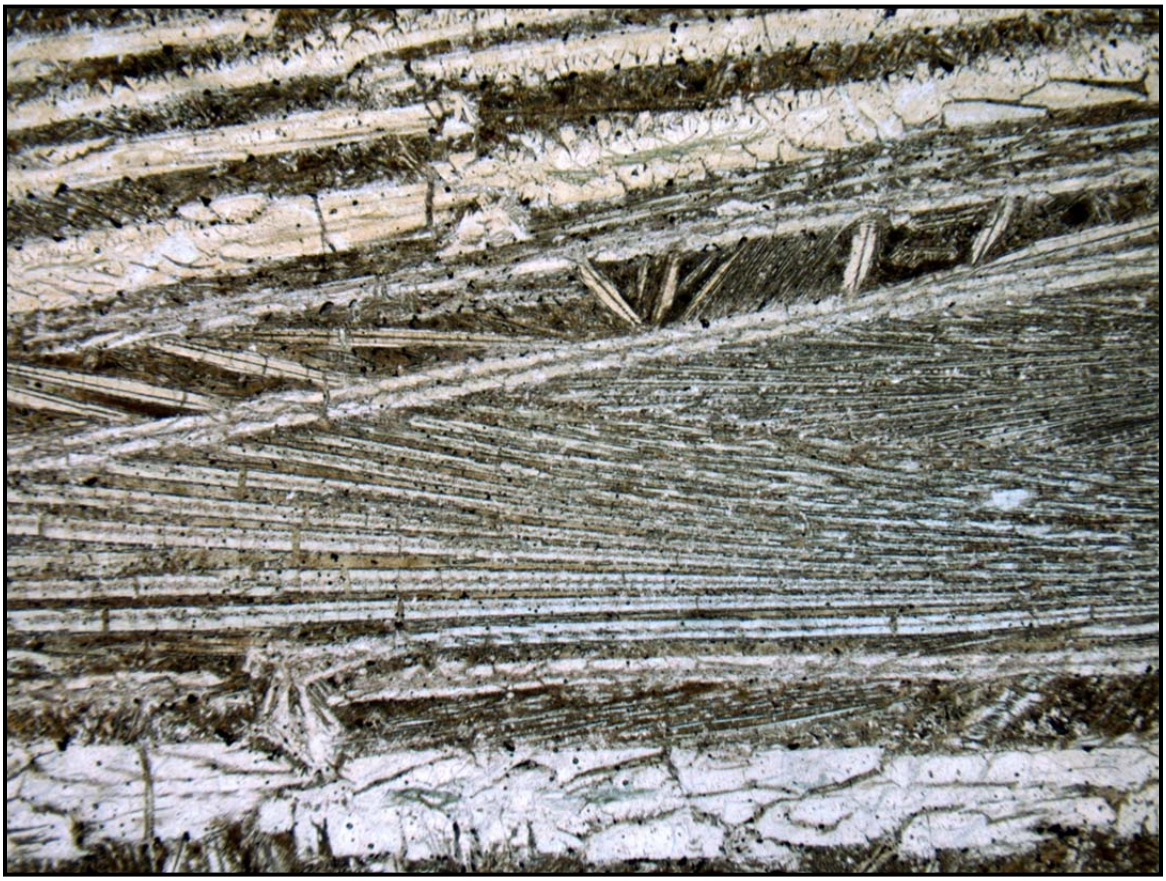

Brian D. Connolly

GEOL394H Senior Thesis
Advisor: Dr. Igor S. Puchtel
Spring 2011

Table of Contents

Abstract

High-precision highly siderophile element (HSE: Os, Ir, Ru, Pt, Pd, Re) abundances, Re-Os isotopic compositions, as well as major, minor, and trace lithophile element abundances are determined for a suite of remarkably fresh komatiite samples from the Weltevreden Formation of the Barberton Greenstone Belt, South Africa. The komatiite lavas examined are calculated to have contained an average of 31% MgO upon emplacement. This is one of the most MgO-rich lavas currently known to have erupted onto Earth's surface. Based on the partitioning behavior of V, and the highly incompatible element depleted nature of the lava, anhydrous melting for the Weltevreden Formation komatiites is inferred. The high calculated liquidus temperatures of the emplaced komatiite magmas of *ca*. 1600ºC require an unusually hot (>1800ºC) mantle source for the lavas, >200ºC hotter than for the ambient contemporaneous mantle. These observations are consistent with formation of the Weltevreden komatiites in a deep mantle plume. A precise Re-Os isochron age of 3266 ± 8 Ma ($2\sigma_m$), as well as HSE abundances for a set of whole-rock komatiite samples and an olivine separate are obtained. These data are used to estimate the absolute and relative HSE abundances of the early Archean mantle. The Weltevreden komatiite source is shown to have abundances that are similar to those in the sources of other late Archean komatiites, and *ca*. 80% of those in the modern upper mantle. If the HSE budget of the terrestrial mantle was established as a result of accretion of large planetesimals after the last major interaction between the core and the mantle, this study shows that the late accreted material must have been thoroughly homogenized within the mantle by 3.3 Ga.

List of Figures

List of Tables

I. Introduction

1.1 Komatiites

Komatiites are high-MgO (>18%) lavas that form via high degrees of partial melting of the mantle upon ascent (Arndt, 1977; 2008). Komatiites ruled the Earth in the Archean, then became scarce in the Proterozoic, and almost non-existent in the Phanerozoic. Ever since komatiites were first described more than 40 years ago (Viljoen and Viljoen, 1969a, 1969b), these rocks have been extensively used to determine mantle characteristics due to their ability to accurately record the approximate compositions of their respective melting source regions (e.g., see review in Arndt et al., 2008). Due to the fact that komatiites form at high degrees of partial melting, they can extract large proportions of HSE from their mantle sources (Barnes et al., 1985; Keays, 1995). Komatiitic magmas have low viscosities and ascend rapidly (Huppert and Sparks, 1985), and therefore undergo little to no differentiation prior to emplacement. This provides a mechanism for sampling average mantle that is not possible with lower degree melts. In addition, the relatively high abundances of HSE in komatiitic liquids make these elements much less prone to alteration by mantle or crustal contamination. Finally, differentiation within komatiite lava flows often caused fractionation of Os from Re, and HSE from MgO. The resulting range in Re/Os and HSE abundances throughout komatiitic lava flows allows for the generation of isochrons, which can be used to obtain precise chronological information, assess closed-system behavior of the HSE, and precisely determine initial Os isotopic compositions and time-integrated Re/Os. The Os isotopic data, combined with correlations between MgO and HSE, can also be used to calculate the HSE abundances in mantle sources of komatiitic lavas.

1.2 Highly siderophile elements

Highly siderophile elements have an affinity for molten iron and, to a lesser degree, for sulfides (Barnes et al., 1985; Walker et al., 2000). These elements therefore partition themselves into the core during planetary differentiation. Absolute and relative abundances of HSE in the mantle can be used to study many mantle processes such as Earth's primary differentiation (Righter, 2003), continued accretion following core formation (Morgan et al., 1981; Morgan, 1985; 1986), and differentiation of the mantle (Walker et al., 1989). Unfortunately, most mantle materials that have been studied for HSE and Os isotopic compositions have been heavily processed via melt extraction/crystal fractionation and fluid- or melt-rock interactions and it has been problematic to constrain the HSE abundances in their respective mantle domains (e.g., Rehkämper et al., 1999a; 1999b; Becker et al., 2006; Lorand et al., 2009).

Over the last 25 years, HSE abundances coupled with Os isotopic systematics have been used to characterize the geochemical history of komatiitic mantle reservoirs (Barnes et al., 1985; Crocket and MacRae, 1986; Brügmann et al., 1987; Walker et al., 1988). Since then, tremendous advances in analytical techniques have made possible the precise determination of Os isotopic compositions and HSE abundances in Archean and post-Archean komatiite systems (e.g., Walker et al., 1991, 1999; Shirey and Barnes, 1994; Shirey, 1997; Puchtel et al., 2004a, 2004b, 2009a, 2009b). However, despite the substantial advances, the high-quality database for early Archean komatiite systems remains limited to the *ca*. 3.6 Ga Schapenburg Greenstone Remnant (Puchtel et al., 2009a). The lack of research focused on HSE abundances and Os isotopic systematics is due in part to the poor state of preservation of the early Archean geologic record in general and

the komatiite record in particular, and in part due to the analytical challenges that this type of study poses.

1.3 Importance of Weltevreden Formation komatiites

Komatiites of the Weltevreden Formation (Fm.) can provide unique insights into the composition of the early Archean mantle. The samples collected from the Weltevreden Fm. are remarkably fresh by Archean standards, retaining much of their primary igneous textures and mineralogy. These relatively pristine komatiites, will further enhance our understanding of early mantle thermal evolution. From the geochemical analysis of these ancient rocks, we can infer mantle temperatures, which can be applied to geophysical models of early Earth evolution. The results of this study will potentially bring understanding to many unanswered questions pertaining to fundamental planetary processes.

1.4 Hypotheses

I. Weltevreden Formation komatiites formed approximately 3.3 billion years ago.
II. By 3.3 Ga, the terrestrial mantle had absolute and relative HSE abundances similar to those in the modern mantle.
III. Weltevreden komatiites formed via anhydrous and high degree, high temperature partial melting, likely in a mantle plume source.

II. Geologic Background, Samples, and Previous Studies

2.1 Geologic background of the Barberton Greenstone Belt

2.1.1 Barberton Greenstone Belt

The Barberton Greenstone Belt (BGB; Fig. 1) in South Africa consists of a succession of supracrustal rocks comprising the so-called Swaziland Supergroup, which ranges in age from *ca.* 3550 to *ca.* 3220 Ma. Komatiites, as a new class of rocks, were discovered and first described here (Viljoen and Viljoen, 1969a, 1969b; Viljoen et al., 1983). The Swaziland Supergroup is made up of three main lithostratigraphic units, ~15 km in total thickness: the lower, mostly volcanic, Onverwacht Group and the upper, predominantly sedimentary, Fig Tree and Moodies Groups (Lowe, 1994, 1999; Lowe and Byerly, 1999, 2007). A major fault zone, the Inyoka Fault, is believed to represent a tectonic-stratigraphic boundary between the northern and southern parts of the BGB (Fig. 1). Throughout the BGB, the Onverwacht Group includes three lower Formations, the Sandspruit, Theespruit, and Komati, which constitute the Tjakastad Subgroup. There are four upper Formations, the Hooggenoeg, Kromberg, Mendon, and Weltevreden, which constitute the Geluk Subgroup (Lowe and Byerly, 1999).

The age of the supracrustal rocks within the Onverwacht Group is well constrained by U-Pb zircon dating. Felsic volcanic rocks from the Theespruit Fm. have Pb-Pb and U-Pb zircon ages of 3544 ± 3 to 3547 ± 3 Ma (Kröner et al., 1996). Felsic volcaniclastic sediments within the Komati Fm. have a zircon U-Pb age of 3482 ± 5 Ma (Armstrong et al., 1990). A tuff in the

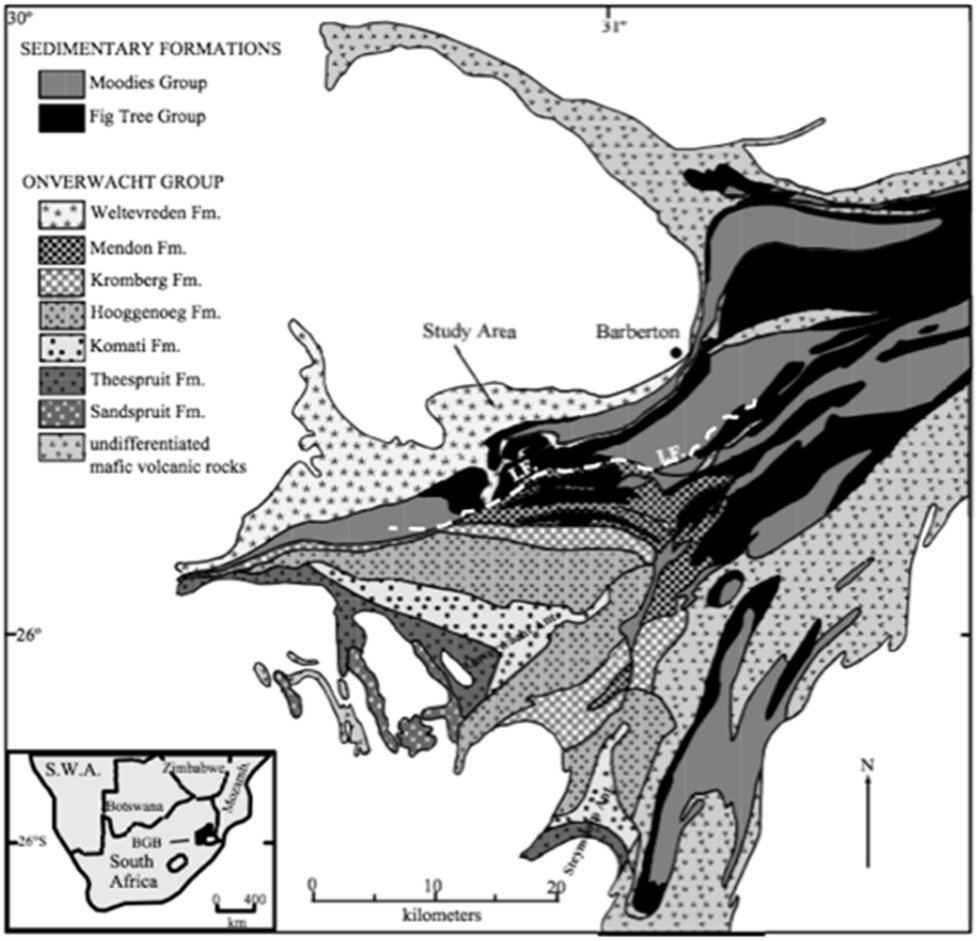

Figure 1. Generalized geologic map of the western half of the Barberton Greenstone Belt, South Africa. Komatiite samples have been collected from several differentiated lava flows from the Weltevreden Formation. The Inyoka Fault (I.F.), highlighted by the dashed line, separates the northern facies from the southern facies (modified after Lowe and Byerly, 1999).

basal part of the Kromberg Fm. has a mean U-Pb zircon age of 3416 ± 5 Ma, whereas zircons from thin felsic ash layers within the Mendon Fm. have a mean age of 3298 ± 3 Ma (Byerly et al., 1996).

Within the Tjakastad Subgroup, komatiites and komatiitic basalts dominate the Sandspruit and Komati Fms., whereas the Theespruit Fm. consists mainly of interlayered komatiite flows and felsic tuffs together with thin bands of chert, metapelite, and sandstone (Viljoen and Viljoen, 1969a; Viljoen et al., 1983). The Mendon Fm. of the Geluk Subgroup is also dominated by komatiites and komatiitic basalts, but is distinct from the Komati Fm. in that it contains abundant shallow-water interflow sediments (Lowe and Byerly, 1999).

2.1.2 Weltevreden Formation

The Weltevreden Formation (Fig. 1) consists of the oldest exposed rocks on the northern facies of the Swaziland Supergroup. The formation is correlative to the upper flows of the Mendon Formation in the southern facies (Lowe and Byerly, 1999). Thickness of the formation is poorly known because the base is not well exposed; however, individual flow units are estimated to range from 10 to 500 m in thickness (Lowe and Byerly; 1999). Komatiitic and basaltic volcanic rocks, peridotitic intrusive rocks, komatiitic tuff, and black and banded chert define the Weltevreden Fm. (Anhaeusser, 1985).

Numerous large, lenticular and layered ultramafic intrusive bodies are present and consist of alternating and repeating units of serpentinized dunite, peridotite, orthopyroxenite, clinopyroxenite, and gabbro (Anhaeusser, 1985). Ultramafic bodies intruded along relatively weak horizons of komatiitic tuffs range from 2 – 60 m thick (Lowe and Byerly, 1999; Stiegler et al., 2008). The komatiitic tuffs have been serpentinized and now consist of fine-grained serpentine, chlorite, amphibole, and talc (Stiegler et al., 2008). A layer of 1 – 10 m thick black and banded chert caps the Weltevreden Fm. (Lowe and Byerly, 1999). The Weltevreden Fm. has not yet been dated directly, but it is older than the overlying Fig Tree Group, which has a minimum age of 3259 ± 5 Ma (Byerly et al., 1996), and is correlated with the Mendon Fm.

2.2 Samples

The set of samples used in this study was provided by our collaborators G. Byerly, N. Ardnt, and C. Robin. These samples came from three differentiated komatiite lava flows, namely SA501, KBA12, and SA564, approximately 65 m-, 25 m-, and 23 m-thick, respectively (Fig. 2). Lava flow SA501 contains fresh olivine grains throughout the top 20 m of the cumulate zone. The remaining 45 m is comprised of serpentinized olivine cumulate. Lava flow KBA12 contains fresh olivine grains within the top 10 m of the lava flow, transitioning into a completely serpentinized olivine cumulate in the lowermost 15 m. Lava flows SA501 and KBA12 have thin spinifex zones, ranging in thickness from 150 cm to 75 cm, respectively. These two flows are stacked, with flow KBA12 directly overlying flow SA501. Lava flow SA564 has a well-preserved upper chilled margin and is separated by a fault from the SA501 and KBA12 series flows. Chilled margins are rarely observed throughout komatiite lava flows, but when present, offer vital information pertaining to the composition of the emplaced lava. The chilled contacts for lava flows SA501 and KBA12 were not found.

Based on observations and petrographic analyses, samples from these rocks can be classified as random olivine spinifex, oriented olivine spinifex, and olivine cumulate lithologies. Cumulate layers consist of relic olivine grains and partially serpentinized olivine (Fig. 3 a-b). The majority of the cumulate samples contain fresh equant olivine grains with serpentinized rims and veins. Olivine is distinguished as having high relief and high birefringence, relative to serpentine. The size of olivine grains range from 0.05 to 1 mm in diameter, with an average size of 0.1 mm. Cumulate chromite is also present within the cumulate and spinifex zone samples. Chromite displays equant, cruciform, and skeletal morphologies. Interstitial pyroxene occurs as fine acicular orthopyroxene crystals rimmed by pigeonite and augite.

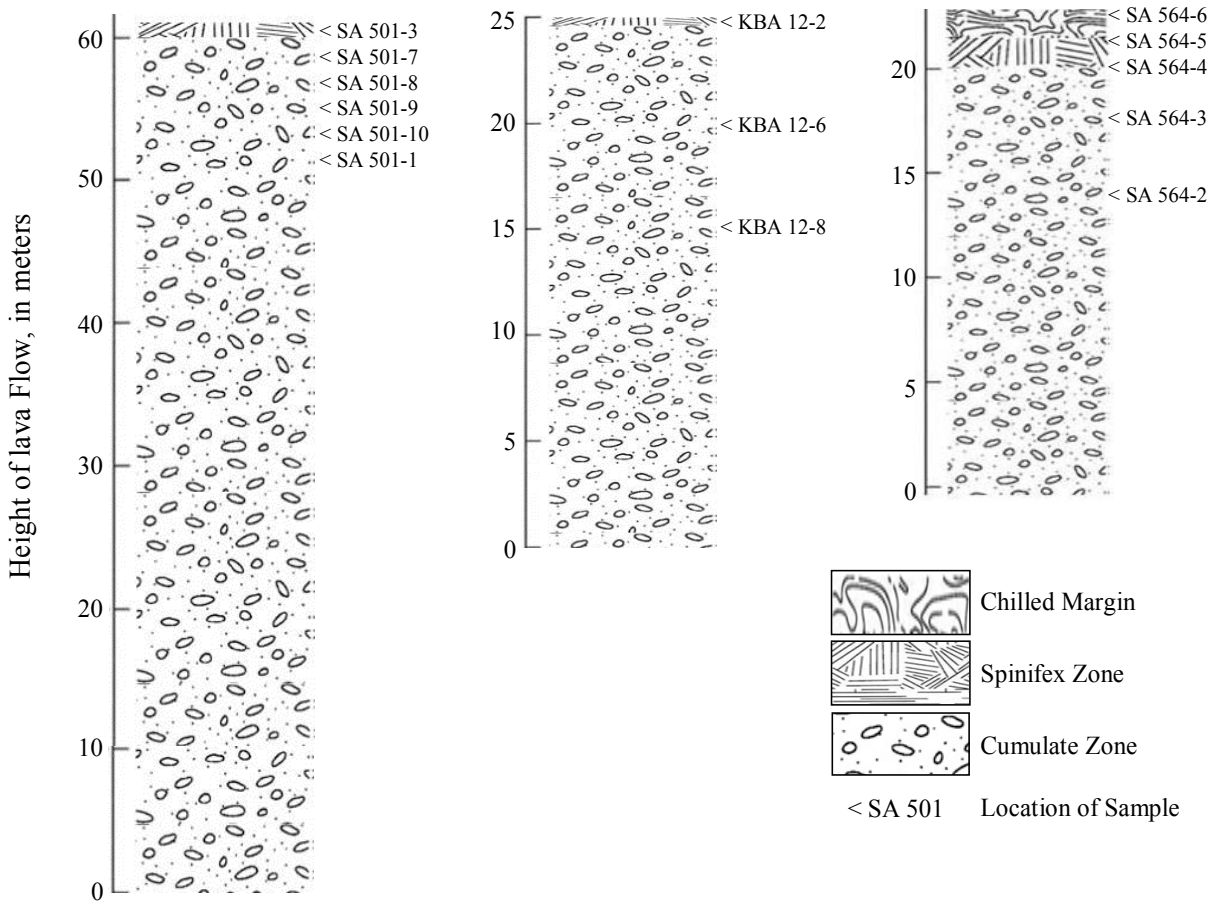

Figure 2. Schematic sections through SA501, KBA12, and SA564 lava flows and location of samples analyzed in this study. Spinifex and chilled margin zones have been slightly exaggerated in order to be visible on sections.

The random spinifex layers contain serpentinized acicular olivine and chromite grains, orthopyroxene, and clinopyroxene (Fig. 3 c-d). The olivine crystals reach ~90 mm in length and have been completely altered to serpentine. Chromites occur as equant cruciform or skeletal grains ranging up to 0.3 mm in size. Acicular pyroxene grains composed of orthopyroxene cores with clinopyroxene rims reach up to 13.5 mm in length.

The quenched chilled upper margin sample (Fig. 3 e-f) contains serpentinized olivine grains within a fine matrix. Serpentine appears around the rims of olivine grains as well as veins within the olivine. Olivine grains reach up to 1 mm in diameter. Chromite also appears as equant cruciform grains ranging up to 0.2 mm in size.

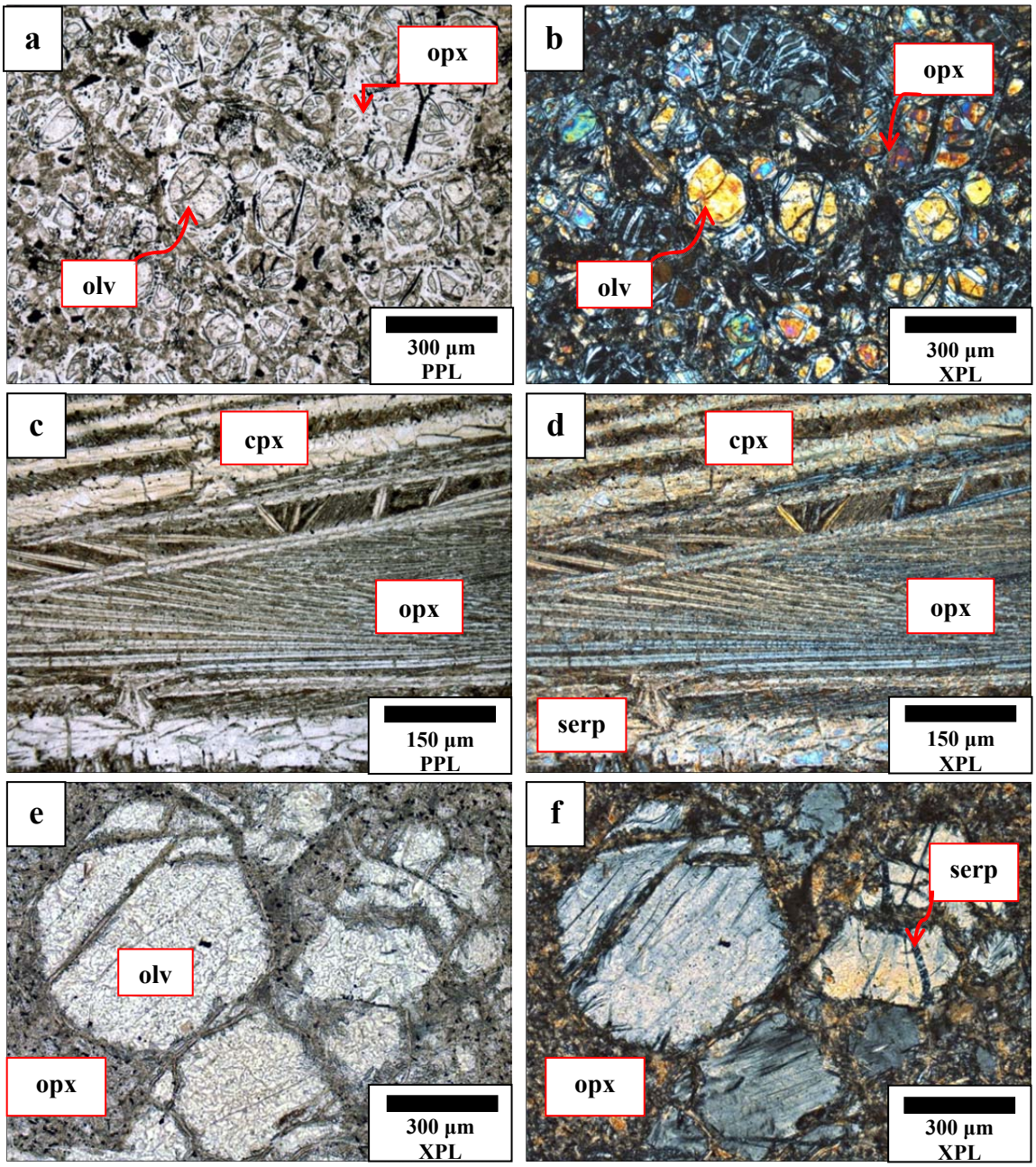

Figure 3. Optical photomicrographs of selected thin sections: (a-b) cumulate zone [SA 564-3], (c-d) random spinifex [KBA 12-2], (e-f) chilled margin [SA 564-6]. olv = olivine, opx = orthopyroxene, cpx = clinopyroxene, serp = serpentinized olivine.

2.3 Previous studies

2.3.1 Komatiites

Viljoen and Viljoen (1969a) first classified komatiites when they discovered ultramafic lavas in the Barberton Mountain Land, South Africa. Viljoen and Viljoen (1969a) described field observations of the region consisting of chilled flow tops, pillow-like structures, and spinifex textures. Chemical analysis of komatiites demonstrated that lavas from the BGB were

magnesium-rich (>18%), having high $CaO:Al_2O_3$ ratios and low incompatible element abundances (Viljoen and Viljoen, 1969b). The current accepted definition of a komatiite is an ultramafic lava or volcaniclastic rock with >18% MgO, whereas komatiitic lava flows containing 9 – 18% MgO are termed komatiitic basalts (Arndt and Nisbet, 1982).

Studies on other shield areas (Canada, Zimbabwe, Australia, India) show the existence of ultramafic volcanic rocks resembling many of the same traits of the Barberton type komatiites (Lowe and Byerly, 1999). Ultramafic volcanic suites from these regions have high MgO contents but show lower $CaO:Al_2O_3$ ratios compared to komatiites from the Barberton region (Arndt et al., 1977; Arndt and Nisbet, 1981). The differences in type lead to the classification of komatiites based on Al contents. Due to Ca-mobilization during alteration, Al/Ti, Ti/Y, and Gd/Yd ratios are now used in addition to CaO/Al_2O_3 to classify komatiites (Chavagnac, 2004; Puchtel et al., 2009a, 2009b). The so-called Al-undepleted, or Munro-type, komatiites are characterized by Primitive Mantle normalized Al/Ti, Ca/Al, Ti/Y, and Gd/Yb that are close to unity. These lavas mostly occur in the late Archean greenstone belts (Ardnt et al., 1977; Arndt and Nisbet, 1981, Puchtel et al., 2009a, 2009b). The Al-depleted/enriched, or Barberton-type, lavas are characterized by depletions or enrichments in Al, Y, and HREE, as compared to Primitive Mantle estimates. These lavas mostly occur in early Archean terrains (Puchtel et al., 2009b).

Komatiite lava flows often differentiate with a cumulate base, a spinifex zone, and a chilled margin flowtop (Fig. 2). The cumulate zone typically contains equigranular polyhedral olivine crystals (Ardnt et al., 2004). A thin zone of aligned foliated olivine crystals may be present, separating the cumulate base from the upper spinifex zones. Spinifex zones are divided into a lower layer of subparallel olivine plates aligned normal to the flow top and an upper layer of randomly oriented olivine plates. Atop the spinifex zone, an upper chilled margin caps the lava flow.

Geochemical analyses conducted on BGB komatiite lava flows indicate that these rocks are magnesium-rich, with MgO ranging between 18 – 50 wt. % (Kareem and Byerly, 2003; Arndt and Nisbet, 2008; Puchtel et al., 2009a). Previous studies conducted on the Weltevreden Formation describe primary mineralogy consisting of olivine, orthopyroxene, pigeonite, augite, and chromite (Kareem, 2005). Kareem and Byerly (2003) state that the olivines from the Weltevreden komatiites have forsterite (Fo) contents that range from 92.5-95.6%, showing higher Fo contents than those reported from komatiites of Abitibi (88.3-93.4% – Arndt, 1977), Belingwe (up to 91.3% – Nisbet et al., 1987), and Barberton Greenstone Belts (90.4-91.3% – Smith et al., 1980), but similar to the olivines reported from the contemporary Commondale Greenstone Belt (96.5% – Wilson et al., 2003).

Komatiites contain low concentrations of incompatible trace elements and therefore are thought to form at high degrees of partial melting, up to as much as 50% in some locations (Sun and Nesbitt, 1978; Arndt et al., 2008). Melting of a solid rock to form magma is controlled by three physical parameters: temperature, pressure, and composition. Minerals have different melting points, therefore, as temperature, pressure, and/or composition change, gradual and incremental melting of a rock occurs. It has been suggested that the formation of komatiites at a high percentage of melting would require mantle temperatures to be 200 – 300°C hotter than those temperatures currently predicted by secular cooling models (Nisbet et al., 1993).

2.3.2 Thermal evolution of the Earth's mantle

Our current understanding of the thermal evolution of the Earth's mantle relies on geochemical, geophysical, and tectonic models. Models of early Earth evolution depend heavily on the geochemical analysis of significantly altered Archean rocks and therefore, cannot fully represent their mantle domains. Secular cooling models indicate the temperature at 3.3 Ga to be *ca*. 1600°C (Richter, 1988). However, recent attempts have been made to adjust thermal evolution models to encompass the current, improved understanding of mantle dynamics (e.g., Korenaga, 2006). By back-projecting Earth's thermal evolution and by adjusting model parameters, Korenaga (2006) showed that early Archean mantle temperatures possibly range from *ca*. 1600°C to an upper limit of 1800°C. More recent secular cooling models indicate early Archean mantle temperatures to range from 1500 to 1700°C (Labrosse and Jaupart, 2007; Herzberg et al., 2010).

2.3.3 Determining the origin of komatiites: wet vs. dry melting

The origin of komatiites is an open and active debate. Komatiites are argued to form by either relatively cold melting of a hydrous mantle (Parman et al., 2001) or by high degree, high temperature anhydrous partial melting (Sun and Nisbet, 1978; Arndt et al., 1998). Cold melting of a hydrous mantle implies a subduction zone setting, whereas high temperatures and anhydrous melting indicates a mantle plume origin. Determining the origin of komatiites has implications for constraining the thermal regime of the Archean mantle and its subsequent evolution.

Advocates of the hydrous melting model of komatiite origin argue that the presence of water reduces the required temperatures of the mantle to more "normal" conditions (Green et al., 1974). Green et al. (1974) demonstrated experimentally that the liquidus of komatiites, in the presence of water, is lowered by as much as 400 K, which, however, would require very high water contents (10 – 20%). Based on geochemical similarity to modern boninites, Parman et al. (2001) proposed that hydrous melting in a subduction zone produced BGB komatiites. Parman et al. (2001) reported that BGB basaltic komatiite compositions overlap those of boninites, showing similar SiO_2 content, comparable trace element abundances, equivalent rare earth element patterns and negative Ti, Nb, and Ta anomalies for a given MgO content.

Opposing arguments state that komatiites originate from a dry, mantle plume source. The main argument against hydrous melting is evident in chemical and isotopic compositions in most komatiites. Most komatiites are interpreted to derive from a source depleted in trace elements (Sun and Nesbitt, 1978). According to Arndt et al. (1998), such depletion would remove water, which is highly incompatible, leaving a dry source.

Canil (1997) reported data for V partitioning between glass inclusions and host olivine in Belingwe komatiites that indicate that the oxidation state of these lavas, as well as several other komatiites, such as those from Abitibi, was very similar to that of present-day plume-derived oceanic island basalts. Vanadium concentrations can therefore be used as a redox indicator, but require knowing how the distribution of V between melt and liquidus phase ($D_V^{ol/liq}$) changes as a function of temperature, composition, and oxygen fugacity (fO_2). For the temperature-compositional range of komatiite crysallization, the major variable controlling $D_V^{ol/liq}$ is fO_2 (Canil, 1997). A range for observed V distribution coefficients for komatiitic magmas has been established for plume-derived (0.025- 0.15) and arc-derived (<0.01) systems (Canil, 1997; Canil, 1999; Canil and Fedortchouk, 2001).

2.3.4 Determining the mantle source characteristics

In order to calculate the absolute abundances of major, minor, trace and HSE in the komatiite sources, we use a projection technique that has been previously applied (Puchtel et al., 2004a, 2004b, Puchtel and Humayun, 2005, Puchtel et al., 2009a, 2009b). This technique is based on the assumption that a mineral phase behaves similarly during low-pressure partial melting in the mantle source as it does during crystallization of the lava upon emplacement. Thus, if an element was incompatible with the residual mineral assemblage during melting that produced that lava, it was also likely to be incompatible with the liquidus mineral assemblage during differentiation of an emplaced komatiitic lava (Puchtel et al., 2009b).

The abundances of elements that are incompatible with the residue should plot on the liquidus lines of descent drawn through the data for the lavas, from which, source concentrations can be calculated for a given MgO content. We will use the accepted MgO content in the Primitive Mantle (PM) established by McDonough and Sun (1995) of 38 wt %. However, because HSE have an affinity for both molten Fe and sulfide, this technique to calculate HSE source abundances requires the complete exhaustion of sulfide in the source during partial melting. Sulfur content at saturation of a mafic lava increases with decreasing pressure, as such, magmas become undersaturated during adiabatic ascent (Mavrogenes and O'Neill, 1999). This could result in differing bulk HSE partition coefficients between partial melting in the mantle source and upon crystallization. Therefore, for this technique to be applicable for determining the HSE composition of the mantle source, complete exhaustion of sulfide from the source must be obtained during partial melting. Sulfide exhaustion occurs if the degree of melting exceeds ~25% (Barnes et al., 1985; Hamlyn et al., 1985; Keays, 1995).

2.3.5 Calculating potential mantle temperature

The maximum potential temperature of the Archean mantle is poorly constrained. Komatiites provide one the most direct ways of determining the mantle temperature during the Archean (Nisbet et al., 1993; Canil, 1997). By using the MgO contents of komatiitic liquids, the maximum potential temperature of the Archean mantle can be derived by back-projecting the temperature of the liquid arriving at the surface to the point at which the liquid left the solid mantle adiabat (Nisbet et al., 1993). It has been established that the Fe/Mg ratio in a basaltic magma is directly related to its liquidus temperature (Roeder and Emslie, 1970; Abbott et al., 1994). If the liquidus temperature (T_{liq}) is the temperature at the top of the convecting mantle, then T_{liq} can be assumed to be directly related to the potential temperature of the mantle (Abbott et al., 1994, Puchtel et al., 1998). Using an olivine-liquid Fe-Mg partitioning coefficient (K_D) equal to 0.30, the FeO/MgO of the olivine can be calculated from that of the liquid composition (Abbott et al., 1994). Absolute concentrations of FeO and MgO in olivine are obtained from a mass balance based on olivine stoichiometry, $(Mg,Fe,Mn,Cr,Ca)_2SiO_4$. The temperature can then be calculated by using

$$\ln K_D Mg = 6921 / T_{liq} + 0.034\,Na + 0.063K + 0.01154\,P - 3.27$$

or

$$T_{liq} = 6921 / \left(\ln K_D Mg + 3.27 - 0.0034\,Na + 0.063K + 0.01154\,P\right),$$

relating temperature to MgO content in the emplaced lava, the MgO content in olivines, and the alkalies (Langmuir et al, 1992; Abbott et al, 1994). The maximum potential temperature can be determined from the maximum eruption temperature (McKenzie and Bickle, 1988; Nisbet et al., 1993) by using:

$$T_{pot} = -1382.5 + 2.8046T_{liq} - 0.000049671\left(T_{liq}\right)^2.$$

By following the protocol of Nisbet et al. (1993) and Abbott et al. (1994) for these relatively pristine Weltevreden Fm. komatiites, we should be able to better constrain estimates of Archean potential mantle temperatures when compared to those previously calculated by using the same methods on other komatiites of similar age. The depth of melting initiation can be estimated by following the protocol of McKenzie and Bickle (1988) which states that depth is exponentially related to T_{pot}:

$$Depth = \exp\left(-95.233 + 0.19401T_{pot} - 0.00012691T_{pot}^2 + \left(2.7982 * 10^8\right)T_{pot}^3\right).$$

The outcomes of this study will benefit thermal evolution models currently relying on mantle temperatures from heavily altered Archean sources. It is noted, however, that any geochemical analysis of Archean mantle rocks must be taken cautiously. Regardless of the relatively pristine condition of these komatiite samples, there is still large uncertainty that these samples can fully represent the mantle source from which they derived. However, with improved analytical techniques, as well as the well-preserved nature of these samples when compared to rocks of similar age and origin, we believe the geochemical study of these komatiites can be extremely beneficial to constraining mantle source characteristics, such as mantle temperatures, and represent one of the best interpretations that can be made to infer such mantle properties.

III. Analytical Techniques

3.1 Sample preparation

The Weltevreden komatiite samples were cut into quarters lengthwise using a diamond saw. Small slabs were cut from the quarters and thin sections were prepared at the Institute of Ore Deposit Geology (IGEM) in Moscow. The remaining parts of the quartered samples were polished on all sides using SiC paper to remove saw marks, washed in deionized water, dried, and crushed in an alumina-faced jaw crusher. A 100- to 150-g aliquot of crushed sample was ground in an alumina shatter box and finely reground in an alumina-faced disk mill to be used for geochemical studies.

3.2 Major and minor elements for whole-rock samples

Major and minor element analyses for whole-rock samples were conducted at Franklin & Marshall College on fused glass discs by using a *Phillips 2404* X-ray fluorescence vacuum mass spectrometer (XRF) equipped with a 4 kW Rh X-ray tube, following the protocol of Mertzman (2000). The typical accuracy of the analyses was ~1% relative for major elements present in

concentrations >0.5% and ~5% relative for the rest of major and for minor elements. Replicate analyses were conducted on both the chilled margin sample (SA564-6) and cumulate samples containing the most magnesian olivine grains (SA501-1 and SA501-8) to ensure the accuracy of these measurements. The chilled margin sample and the most magnesian olive grains are important for calculating mantle source characteristics.

3.3 Highly siderophile elements and Re-Os isotopic systematics

The details of the analytical techniques used to determine the Re-Os isotope compositions and the HSE abundances in the Weltevreden komatiite samples closely follow those described by Puchtel et al. (2009a, 2009b). Approximately 1.5 g of whole-rock sample powder and 400 mg of the pure olivine separate were combined with 6 mL of purged, triple-distilled concentrated HNO_3, 4 mL of triple-distilled concentrated HCl, and appropriate amounts of mixed ^{185}Re-^{190}Os and HSE (^{99}Ru, ^{105}Pd, ^{191}Ir, ^{194}Pt) spikes. These were then sealed in double, internally-cleaned, chilled 25 mL Pyrex™ borosilicate Carius Tubes and heated to 270°C for 96 hours. Osmium was extracted from the acid solution by CCl_4 solvent extraction (Cohen and Waters, 1996), then back-extracted into HBr, followed by purification via microdistillation (Birck et al., 1997). Ruthenium, Pd, Re, Ir, and Pt were separated and purified by using anion exchange chromatography. Average total analytical blanks during the analytical campaign were (in pictograms): Ru: 1.1 ± 0.5 ($\pm 2\sigma_{mean}$, $N = 5$), Pd: 6 ± 2, Re: 0.43 ± 0.17, Os: 0.19 ± 0.05, Ir: 0.45 ± 0.23, and Pt: 11 ± 5. For the whole-rock samples, the total analytical blanks for all HSE constitute less than 0.1% of the total element analyzed.

Osmium isotopic measurements were accomplished via negative thermal ionization mass-spectrometry (NTIMS: Creaser et al., 1991). All samples were analyzed by using a secondary electron multiplier (SEM) detector of a *Thermo Electron Triton* mass spectrometer at the Isotope Geochemistry Laboratory (IGL), University of Maryland-College Park. The measured isotopic ratios were corrected for mass fractionation by using $^{192}Os/^{188}Os = 3.083$. The internal precision of measured $^{187}Os/^{188}Os$ in all samples was better than 0.05% relative. The measured $^{187}Os/^{188}Os$ in 300 pg loads of the in-house Johnson-Matthey Os standard measured during the analytical campaign averaged 0.11377 ± 10 ($\pm 2\sigma_{stdev}$, $N = 23$). This value characterizes the external precision of the isotopic analysis (0.10%) and was used to calculate the true uncertainty on the measured Os isotopic composition for each individual sample. The $^{187}Os/^{188}Os$ ratio measured in each sample was corrected for the instrumental bias relative to the average $^{187}Os/^{188}Os = 0.11378$ measured in the Johnson-Matthey Os standard on the Faraday cups of the *IGL Triton*. The correction factor of 1.0000876 was calculated by dividing this value by the average $^{187}Os/^{188}Os$ measured in the Johnson-Matthey Os standard on the SEM of the same instrument.

The measurements of Ru, Pd, Re, Ir, and Pt were performed at the *IGL* by inductively coupled plasma mass-spectrometry (ICP-MS) by using a *Nu Plasma* instrument with a triple electron multiplier configuration in a static mode. Isotopic mass fractionation was monitored and corrected for by interspersal of samples with standards. The accuracy of the data was assessed by comparing the results for the reference materials UB-N and GP-13 obtained during Igor Puchtel's ongoing analytical campaign (Puchtel et al., 2007; Puchtel et al., 2008) with the results from other laboratories. Concentrations of all HSE and Os isotopic compositions obtained at the *IGL* are in good agreement with the other labs (Becker et al., 2006; Puchtel and Humayun, 2005). Diluted spiked aliquots of iron meteorites were run during each analytical

session as secondary standards. The results from these runs agreed within 0.5% for Re and Ir, and 2% for Ru, Pt, and Pd with fractionation-corrected values obtained from measurements of undiluted samples using Faraday cups of the same instrument with a signal of >100 mV for the minor isotopes.

Therefore, I cite ±2% as uncertainty on the concentrations of Ru, Pt, and Pd, ±0.5% on Re and Ir, and ±0.1% on the concentrations of Os in the whole-rock samples. The uncertainty in the Re concentration was the main source of uncertainty in the Re/Os ratio. For the whole-rock samples, this uncertainty was, thus, estimated to be 0.5%. All regression calculations were performed by using ISOPLOT 3.00 (Ludwig, 2003).

The initial $\gamma^{187}Os$ value was calculated as the per cent deviation of the isotopic composition at the time defined by the isochron relative to the chondritic reference of Shirey and Walker (1998). The average chondritic Os isotopic composition at the time defined by the isochron was calculated by using the ^{187}Re decay constant $\lambda = 1.666 \times 10^{-11}$ year^{-1}, an early solar system $^{187}Os/^{188}Os = 0.09531$, and the present-day average chondritic composition $^{187}Re/^{188}Os = 0.40186$, $^{187}Os/^{188}Os = 0.1270$ (Smoliar et al., 1996; Shirey and Walker, 1998).

All analyses were corrected for loss on ignition (LOI). As water is introduced to the mineral assemblages, it is necessary to re-calculate the abundances of each element on an anhydrous basis. This is conducted by normalizing each element to a specific correction factor estimated for each sample.

3.4 Major, minor and trace element analyses of olivine grains

Major and minor element analyses of olivine grains were performed on polished thin sections by using the *JEOL JXA-8900R* electron probe microanalyzer (EPMA) at the University of Maryland, College Park. Operating conditions were 15 keV accelerating potential and 20 nA focused electron beam current and a 10 μm spot size. Analyses of the in-house standard, San Carlos olivine, indicates that external precision (2σ) are SiO_2 (0.3%), FeO (0.7%), MgO (0.2%), CaO (4.7%), NiO (3.0%), MnO (7.0%) and Cr_2O_3 (30%).

Transition metal analyses of the most magnesian olivine grains were completed via laser ablation inductively-coupled plasma mass spectrometry (LA-ICP-MS) following the analytical procedures of Arevalo and McDounough (2008). The reliability of in-situ laser ablation methods for measuring trace elements in geologic materials have been previously validated through numerous analytical studies (e.g. Pearce et al., 1997; Norman et al., 1998; Jochum et al., 2005). The samples examined during this study were analyzed by using a New Wave frequency-quintupled Nd-YAG laser (200 nm) coupled to a *Thermo Finnigan Element 2* single-collector ICP-MS at the University of Maryland. When compared to analyses of in-house standards (BHVO-2G and NIST-610), the analyses indicate that precision and accuracy were better than 1-3% relative for most elements.

IV. Results

4.1 Major, minor, trace elements in the emplaced lava

The major, minor, and rare earth element (REE) data for the Weltevreden are presented in Table I and plotted on the variation diagrams in Figure 4. The PM-normalized REE abundances in the lavas are presented in Table II and plotted in Figure 5. The MgO abundances in whole-

Table I.
Major (wt. %) and minor (ppm) element data for Weltevreden komatiite whole-rock samples and olivine separate.

Sample	SiO_2	TiO_2	Al_2O_3	Fe_2O_3	MnO	MgO	CaO	Na_2O	K_2O	P_2O_5	Cr	V	Co	Ni
Chilled Margin														
SA564-6A	46.5	0.186	5.35	10.8	0.16	30.5	5.67	0.07	0.03	0.03	2640	115	93	1722
SA564-6B	45.9	0.185	5.30	10.7	0.16	31.3	5.59	0.05	0.03	0.02	3046	118	100	1952
Spinifex Zone														
SA501-3	47.7	0.184	5.29	10.15	0.15	30.5	5.18	0.09	0.12	0.02	2454	108	95	1561
SA564-4	47.7	0.195	5.83	9.96	0.17	28.8	6.57	0.08	0.10	0.02	2430	120	98	1396
SA564-5	47.8	0.174	5.08	10.05	0.14	31.3	4.65	0.08	0.09	0.02	2559	103	98	1608
KBA12-2	48.0	0.185	5.70	10.84	0.16	28.9	5.37	0.08	0.08	0.02	2901	125	100	1445
Cumulate Zone														
SA501-1A	45.0	0.100	2.68	7.18	0.08	42.8	1.37	0.08	0.02	0.01	2182	60	99	2584
SA501-1B	45.4	0.101	2.58	7.64	0.08	42.6	0.73	0.04	0.02	0.01	1969	58	100	3063
SA501-7	45.7	0.111	2.81	6.39	0.09	41.7	2.49	0.07	0.03	0.01	2090	67	117	2615
SA501-8	46.0	0.111	2.91	6.56	0.09	42.3	1.52	0.07	0.04	0.02	2089	64	96	2789
SA501-9	44.9	0.110	2.91	7.44	0.09	42.1	1.74	0.07	0.03	0.01	2214	63	101	2532
SA501-10	45.5	0.107	2.82	7.28	0.09	41.5	1.89	0.08	0.03	0.01	1998	58	91	2423
SA564-2	43.4	0.098	2.92	9.43	0.14	41.0	2.16	0.07	0.02	0.01	3313	60	116	2331
SA564-3	43.5	0.098	2.75	9.34	0.13	41.4	1.88	0.08	0.02	0.02	3215	58	119	2377
KBA12-6	44.5	0.110	2.84	8.24	0.11	40.7	2.83	0.07	0.01	0.01	2132	70	120	2450
KBA12-8	45.0	0.100	2.52	8.15	0.10	42.0	1.35	0.07	0.02	0.01	2195	58	109	2648
Olivine Separate														
SA501-1OL	41.2	0.001	0.001	5.39	0.07	52.5	0.16	N/A	N/A	N/A	1464	4.8	N/A	3353
Standard														
BCR-1	53.4	2.28	13.8	14.1	0.20	3.69	7.17	3.22	1.80	0.36	46	385	44	45
BCR-1 GeoRef[1]	54.3	2.25	13.7	13.5	0.19	3.57	7.14	3.28	1.71	0.36	13	411	37	12

[1]Accepted values for BCR-1 standard (USGS: Flanagan, 1976).

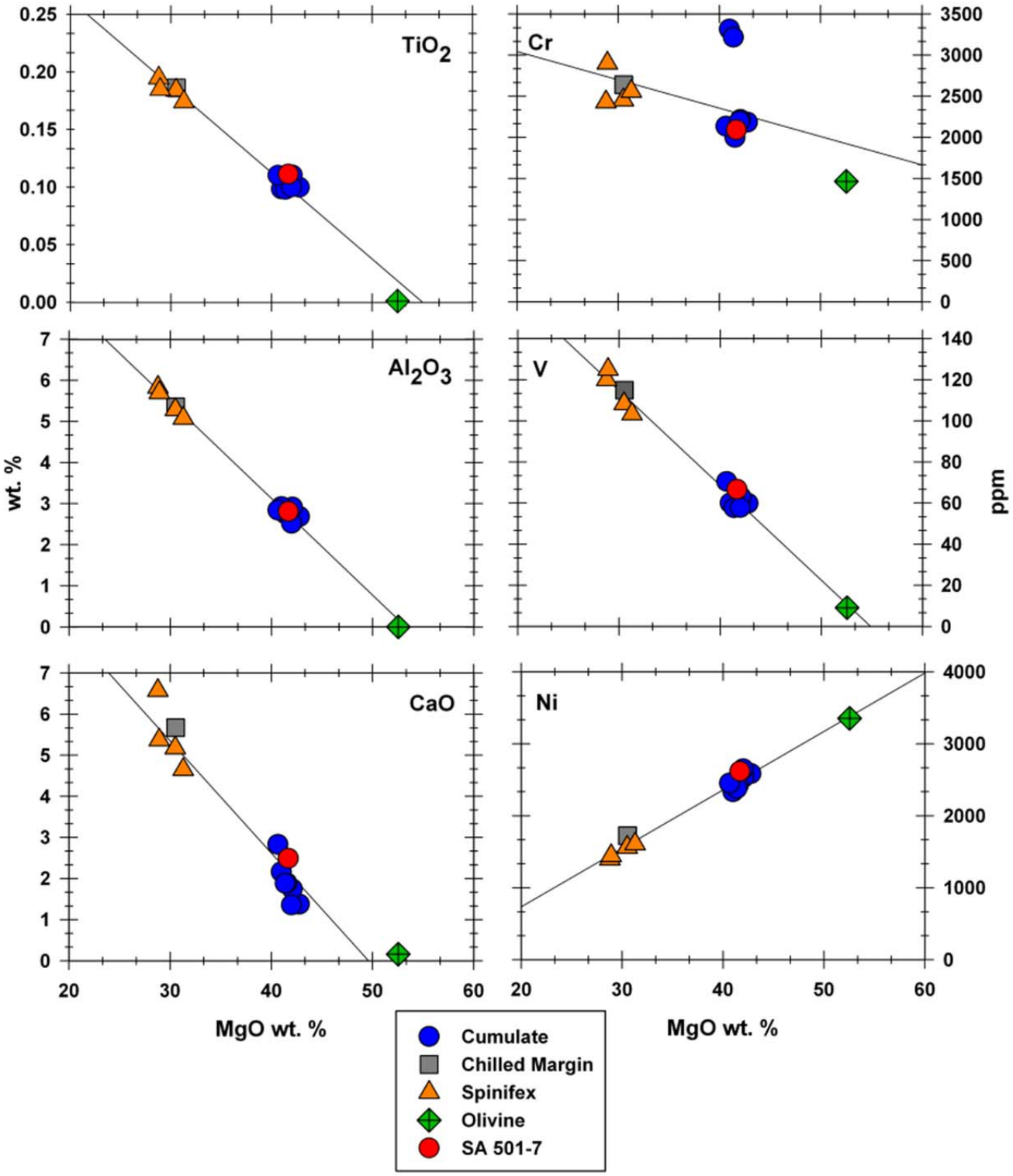

Figure 4. Variations of selected major and minor elements vs. MgO abundances in whole-rock komatiite samples and an olivine separate from the Weltevreden Formation. Error bars are smaller than the size of the symbols.

Table II.
Primitive mantle-normalized incompatible lithophile trace element abundances in the Weltevreden komatiite emplaced lava and calculated Weltevreden mantle source.

	Th	U	Nb	Ta	La	Ce	Nd	Sm	Hf	Zr	Ti	Eu	Gd	Dy	Y	Er	Yb	Lu
Emplaced Lava	0.29	0.51	0.61	0.63	0.62	0.73	0.86	0.95	0.93	0.98	1.1	1.2	1.1	1.2	1.3	1.2	1.2	1.3
Welt. Source	0.19	0.38	0.43	0.43	0.43	0.49	0.58	0.65	0.63	0.66	0.68	0.83	0.74	0.80	0.85	0.84	0.86	0.90

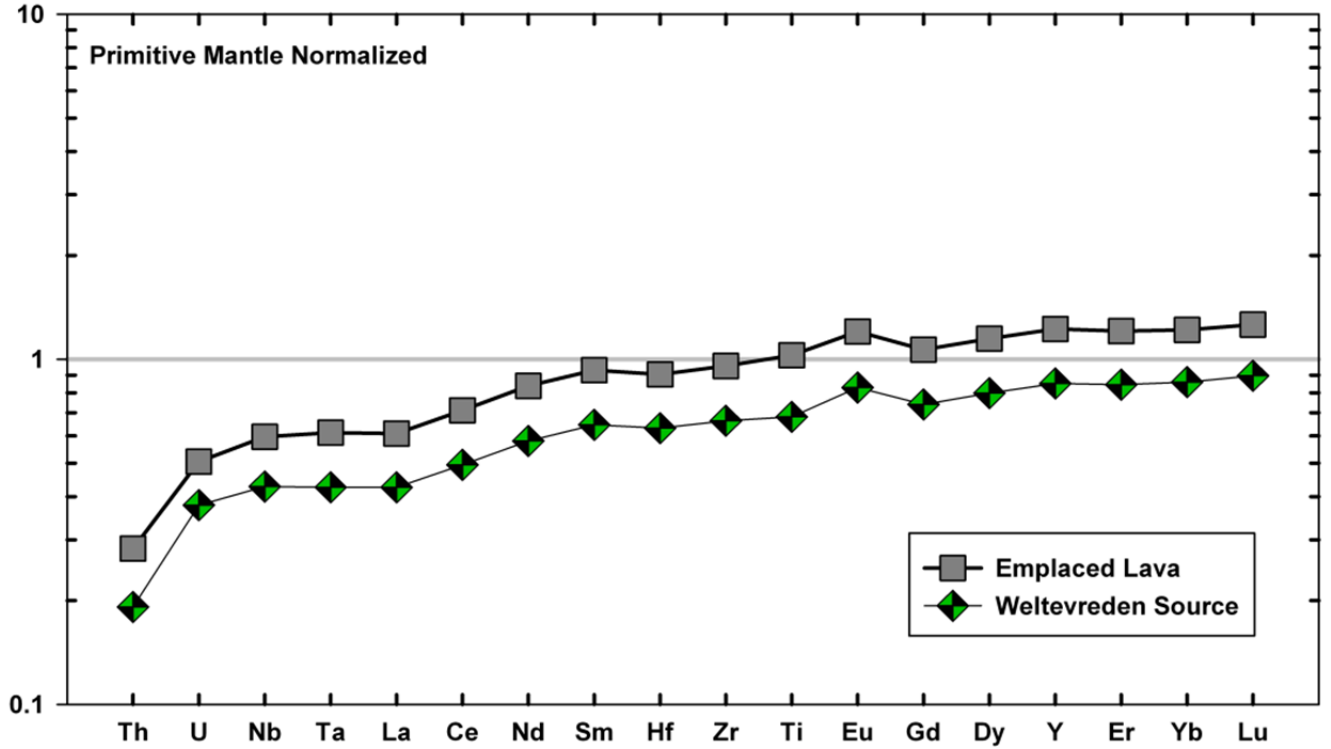

Figure 5. Primitive mantle-normalized (Hoffman, 1988) incompatible lithophile element abundances in the Weltevreden emplaced komatiite lava and calculated mantle source. Error bars are smaller than the size of the symbols.

rock samples vary in a narrow range within the analyzed parts of both the spinifex (28.8 and 31.3%) and the cumulate zones (40.7-42.7%) of the lava flows, and the only available chilled margin sample (SA564-6), contains an average 30.9 ± 0.4 wt.% MgO between the two replicates.

The compatible and incompatible elements both behave similarly to typical komatiite differentiation fashion. When plotted against MgO, the data for Al_2O_3, TiO_2, V, and REE define tight trends, corresponding to olivine control lines, intersecting the MgO axes at an average of 54.1 ± 1.0% ($2\sigma_{mean}$). This is consistent with immobile behavior of these components. The CaO data plot on a steeper trend that does not pass through the olivine composition, instead, intersects the MgO axis at 47.7 ± 1.8%. This implies typical mobility of Ca during post-magmatic alteration of the komatiite lava flow.

The data for Cr also form a trend with a negative slope, indicating that Cr was incompatible with the fractionating mineral assemblage. This trend is somewhat skewed by the high Cr content in cumulate samples SA564-2 and SA564-3, which apparently contain a small amount of cumulus chromite, indicating fractionation of minor chromite in the Weltevreden lava flows. The Ni vs. MgO data define a positive trend indicating the typical compatible behavior of Ni during lava differentiation. The trend passes through the cumulate olivine composition, indicating olivine control over the variations of Ni.

The chilled margin sample is depleted in LREE ($La/Sm_N = 0.66$) and is slightly enriched in HREE ($Gd/Yb_N = 0.88$), which, together with the average elevated PM-normalized $(Al_2O_3/TiO_2)_N = 1.24 \pm 0.05$, allows us to classify these lavas as Al-enriched (Nesbitt and Sun, 1976).

4.2 Composition of the emplaced komatiite lava

Precise determination of the MgO contents of the emplaced komatiite lava is crucial for evaluating the potential mantle temperature of magma generation, and, ultimately, for calculating the absolute and relative lithophile and HSE abundances in the mantle source. We used several independent techniques to calculate the MgO contents of the emplaced komatiite lavas for the Weltevreden flows. First, we used the composition of the upper chilled margin to represent the composition of the emplaced lava. The chilled margin sample is usually a good proxy, as long as it does not show any evidence of post-magmatic disturbance of its major and trace element chemical composition. As stated above, this is represented by the sample SA564-6, which contains 30.9 ± 0.4 wt.% MgO. Second, we used a well-established relationship between the composition of the cumulate olivine and that of the liquid it crystallized from (Roeder and Emslie, 1970; Beattie et al., 1991; Puchtel et al., 2009a, 2009b). The average maximum MgO and minimum FeO contents of the cores of olivine cumulate grains in the Weltevreden flows are 52.6 ± 0.1% and 4.94 ± 0.11% (N=40, $2\sigma_{mean}$), respectively. These olivine compositions can be shown to be in equilibrium with a komatiite liquid containing 31.8 ± 0.7 ($2\sigma_{mean}$) MgO.

The two independent methods, therefore, give consistent results that are identical within the uncertainty. The average MgO contents of the emplaced komatiite lava is, thus, calculated to be 31.6 ± 0.9 wt.% MgO ($2\sigma_{mean}$). These results indicate that the Weltevreden komatiites are amongst the most magnesian komatiite lavas currently known to have erupted on the Earth's surface.

Table III.
HSE abundances (ppb) and elemental ratios in the Weltevreden komatiite whole-rock samples and olivine separate.

Sample	Re	Os	Ir	Ru	Pt	Pd	MgO	LOI	Re/Ir	Os/Ir	Ru/Ir	Pt/Ir	Pd/Ir	Re/Os	Pt/Os
Chilled Margin															
SA564-6	0.345	1.35	1.41	6.56	9.12	7.05	30.5	8.91	0.245	0.957	4.65	6.47	5.00	0.256	6.76
Spinifex Zone															
SA501-3	0.333	1.49	1.56	5.94	8.58	6.60	30.5	7.80	0.213	0.955	3.81	5.50	4.23	0.223	5.76
SA564-4	0.357	1.05	1.13	6.25	9.52	7.46	28.8	7.89	0.316	0.929	5.53	8.42	6.60	0.340	9.07
SA564-5	0.284	1.46	1.45	5.67	7.78	6.14	31.3	8.42	0.196	1.007	3.91	5.37	4.23	0.195	5.33
KBA12-2	0.339	1.21	1.30	6.05	8.89	6.99	28.9	8.08	0.261	0.931	4.65	6.84	5.38	0.280	7.35
Cumulate Zone															
SA501-1	0.169	11.9	10.6	6.28	4.32	3.31	42.8	10.0	0.0159	1.12	0.592	0.408	0.312	0.0142	0.363
SA501-7	0.284	1.18	1.10	5.48	4.98	3.98	41.7	10.1	0.258	1.07	4.98	4.53	3.62	0.241	4.22
SA501-9	0.187	1.12	1.05	5.29	4.74	3.67	42.1	9.79	0.178	1.07	5.04	4.51	3.50	0.167	4.23
SA501-10	0.173	7.07	6.00	5.49	4.54	3.53	41.5	6.85	0.0288	1.18	0.915	0.757	0.588	0.0245	0.642
SA564-2	0.154	2.89	2.92	9.06	4.37	3.34	41.0	8.73	0.0527	0.990	3.10	1.50	1.14	0.0533	1.51
SA564-3	0.072	3.32	3.42	8.98	4.55	3.32	41.4	8.37	0.0211	0.971	2.63	1.33	0.97	0.0217	1.37
KBA12-6	0.162	4.35	3.98	5.59	4.34	3.46	40.7	9.36	0.0407	1.09	1.40	1.09	0.869	0.0372	1.00
KBA12-8	0.122	4.70	4.39	6.04	3.89	2.93	42.0	10.30	0.0278	1.07	1.38	0.886	0.667	0.0260	0.828
Olivine Separate															
SA501-1 OL	0.018	8.55	7.43	5.92	1.89	0.457	53.00	0.00	0.002	1.15	0.80	0.25	0.06	0.002	0.22

4.3 Highly siderophile elements abundances in the emplaced lava

The HSE abundances obtained in this study for the Weltevreden Formation are presented in Table III and plotted as CI chondrite-normalized (using average Orgueil values from Horan et al., 2003) abundances in Figure 6. These data are also plotted against MgO in Figure 7. The Os and Ir abundances in the lava flows vary in a wide range between 1.0 and 12 ppb and were controlled by fractionation of olivine and an Os-Ir rich phase, similar to their younger counterparts (e.g., Puchtel and Humayun, 2001; Puchtel et al., 2004b; Puchtel et al., 2009b). Ruthenium shows minimal variance during olivine fractionation, indicating that the bulk differentiation partition coefficient for Ru was close to unity. It is also evident that the Ru variation is both controlled by olivine and by chromite. Samples SA564-2 and SA564-3 show higher abundances of Ru, consistent with the increased Cr (and, thus, chromite) content in these samples. Rhenium, Pt, and Pd show strong negative correlations with MgO, which is evidence for their typical incompatible behavior during komatiite lava differentiation and immobility during lava alteration. Cumulate samples (SA501-7 and SA564-3), plot well off the regression line for Re. This indicates that these samples likely experienced later movement of Re during post-magmatic alteration.

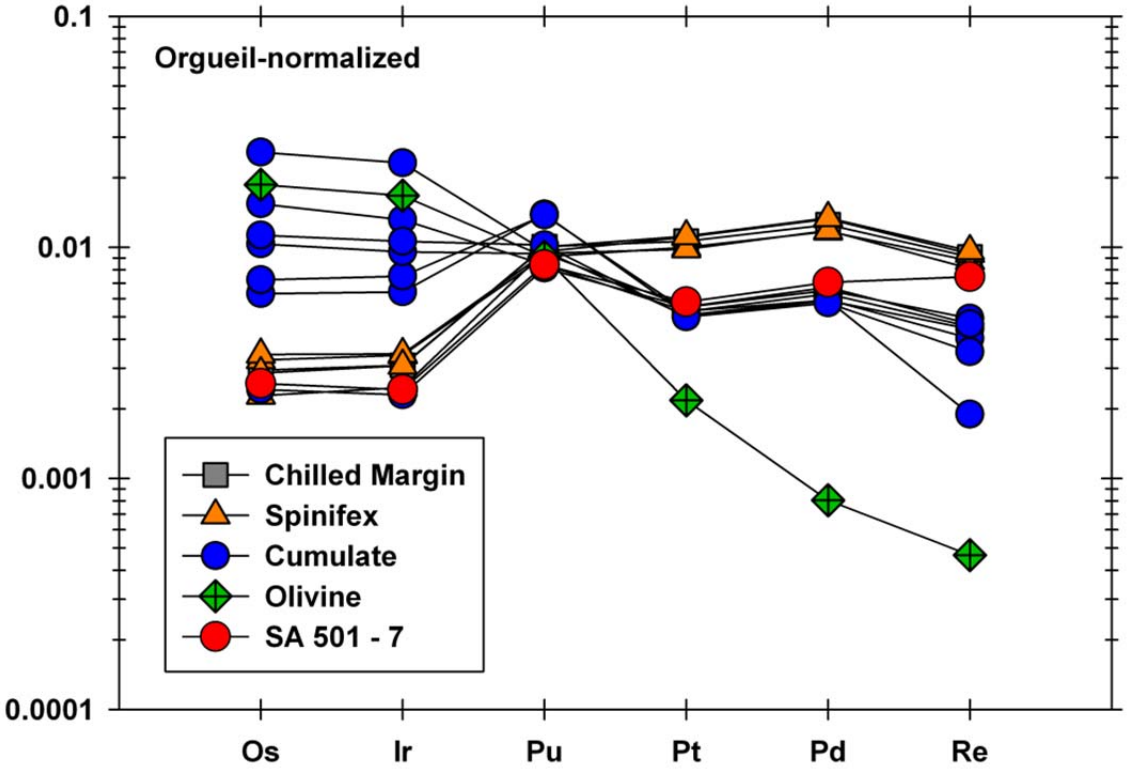

Figure 6. CI chondrite-normalized (Horan et al., 2003) HSE abundances in whole-rock samples and an olivine separate from the Weltevreden Formation. Error bars are smaller than the size of the symbols.

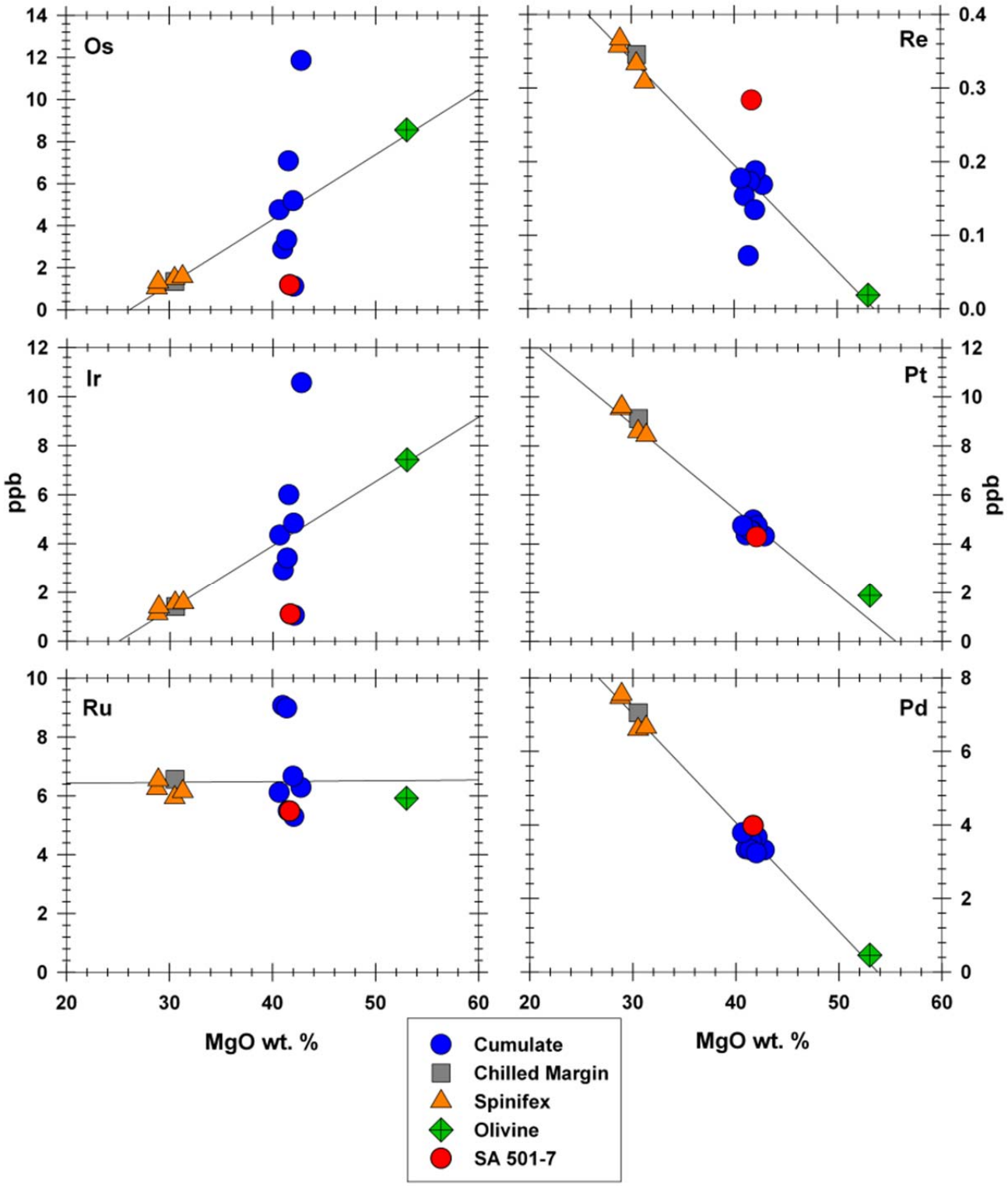

Figure 7. Variations of HSE vs. MgO abundances in whole-rock komatiite samples and an olivine separate from the Weltevreden Formation. Sample SA501-7 is highlighted in red. Error bars are smaller than the size of the symbols.

The HSE abundances in the emplaced lavas, calculated from the ISOPLOT regressions for each element using the MgO content in the emplaced lavas are shown in Figure 8 and these data are presented in Table IV. The HSE abundances for the emplaced lava of the Weltevreden komatiites are (ppb): 0.34 Re, 1.35 Os, 1.41 Ir, 6.56 Ru, 9.07 Pt, and 7.05 Pd. By using the projection technique described above which follows the protocol of (Puchtel et al., 2004a, 2004b; Puchtel et al., 2009a, 2009b), we can determine the Weltevreden source characteristics, with respect to HSE, with large uncertainties, by projecting to the accepted MgO (38.0 wt. %) content in the Primitive Mantle (McDonough and Sun, 1995). As such, the calculated mantle source characteristics for the Weltevreden Fm. are (ppb): 0.223 Re, 0.2.66 Os, 2.78 Ir, 7.21 Ru, 5.97 Pt, and 4.67 Pd. The HSE abundances in the Weltevreden source are similar to those in an average late Archean komatiite source and the total calculated abundances are 80% of those in the modern PM-estimate of (Becker et al., 2006). These data indicate that by 3.3 Ga, HSE were largely homogenized within the mantle on the scale of mantle domains sampled by Weltevreden komatiites, which is consistent with my second hypothesis.

4.4 Re-Os isotopic data

The Re-Os isotopic data for the Weltevreden komatiites are plotted on the Re-Os isochron diagram in Figure 9 and presented in Table V. The Re-Os data for twelve whole-rock samples and an olivine separate define a precise isochron with an age of 3266 ± 8 Ma and a near-chondritic initial $^{187}Os/^{188}Os = 0.10440 \pm 5$ ($\gamma^{187}Os = -0.14 \pm 0.05$). This value represents our best estimate of the initial $^{187}Os/^{188}Os$ in the source of the Weltevreden komatiites. Assuming an early solar system initial $^{187}Os/^{188}Os = 0.09531$ (Shirey and Walker, 1998) and the ^{187}Re decay constant $\lambda = 1.666x10^{-11}$ year^{-1} (Smoliar et al., 1996), it is calculated that the source of the Weltevreden komatiites would have evolved from 4558 Ma to its initial $^{187}Os/^{188}Os = 0.10440$ at 3266 Ma with a time-integrated $^{187}Re/^{188}Os = 0.396 \pm 2$. This value is only slightly lower than the time-integrated $^{187}Re/^{188}Os$ in an average late Archean komatiite source of 0.411 ± 9 (Puchtel et al., 2009b) and is identical, within the uncertainty, to the $^{187}Re/^{188}Os = 0.415 \pm 6$ in the chondritic reference of Shirey and Walker (1998).

Cumulate sample (SA501-7) plots well below the regression line; its high Re/Os is not supported by the respective ingrowth of ^{187}Os and is likely due to late enrichment in Re. This sample likely experienced post-magmatic alteration sometime after emplacement and was therefore not included into regression calculations. As stated above, cumulate sample (SA564-3), which also showed movement of Re likely caused by alteration, still plots well on the Re-Os isochron (Fig. 9). This indicates that this sample experienced movement of Re before the respective ingrowth of ^{187}Os.

Table IV.
HSE abundances in the emplaced lava for Weltevreden Formation and calculated mantle source HSE abundances compared to Average Late Archean sources and PUM estimates.

HSE	Emplaced Lava (this study)	±2σ	Welt. Mantle Source (this study)	±2σ	Avg Late Archean[1]	±2σ	PUM[2]	±2σ
Re	0.34	0.03	0.220	0.02	0.528	0.08	0.35	0.02
Os	1.35	0.01	2.66	0.26	1.83	0.14	3.9	0.09
Ir	1.41	0.03	2.78	0.27	1.64	0.13	3.5	0.40
Ru	6.56	0.13	7.21	0.14	5.54	0.47	7.0	0.12
Pt	9.07	0.62	5.97	0.41	10.1	0.66	7.6	0.21
Pd	7.05	0.49	4.67	0.32	9.82	0.65	7.1	0.31

[1]Puchtel et al., 2009b
[2]Becker et al., 2006

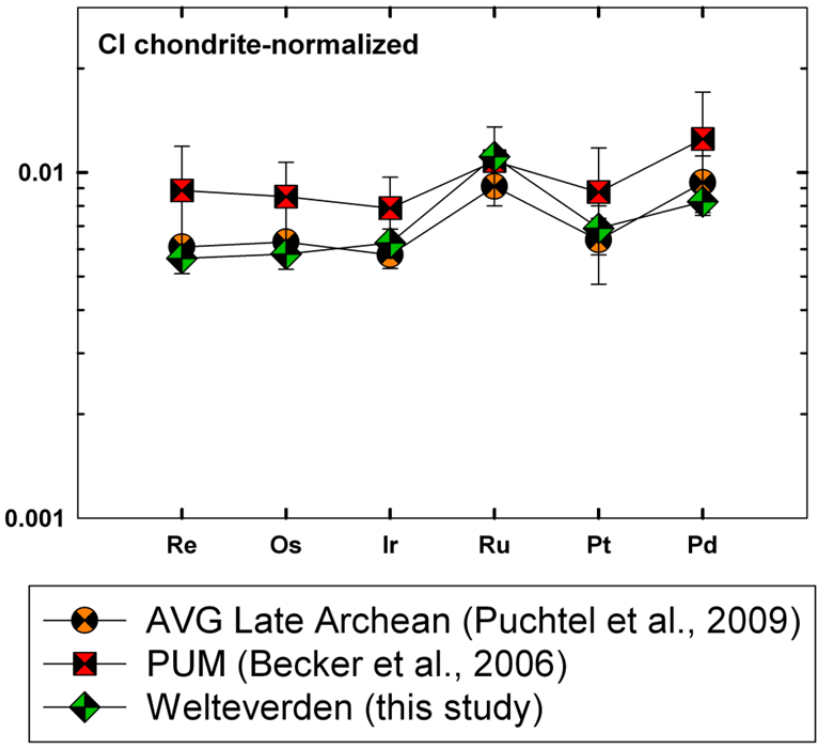

Figure 8. CI chrondrite-normalized (Horan et al., 2003) HSE abundances in the calculated Weltevreden komatiite source compared to an average late Archean komatiite source of (Puchtel et al., 2009b) and a PUM estimate of (Becker et al., 2006). Error bars are reported as ±2σ deviation.

Table V.
Re-Os isotopic data for the Weltevreden komatiites.

Sample	Re	Os	$^{187}Re/^{188}Os$	±2σ	$^{187}Os/^{188}Os$	±2σ	$^{187}Os/^{188}Os(i)$	$^{187}Os/^{188}O(i)_{CH}$	$\gamma^{187}Os(T)$
Chilled Margin									
SA564-6	0.3172	1.238	1.242	0.0062	0.1739	0.0002	0.1044	0.1045	-0.10
Spinifex Zone									
SA501-3	0.3088	1.384	1.080	0.0054	0.1649	0.0002	0.1045	0.1045	-0.07
SA564-4	0.3306	0.9713	1.655	0.0083	0.1969	0.0002	0.1044	0.1045	-0.15
SA564-5	0.2843	1.457	0.9435	0.0047	0.1571	0.0002	0.1043	0.1045	-0.19
KBA12-2	0.3391	1.214	1.355	0.0068	0.1803	0.0002	0.1045	0.1045	-0.04
Cumulate Zone									
SA501-1	0.1532	10.77	0.0682	0.0003	0.1082	0.0001	0.1043	0.1045	-0.19
SA501-7*	0.2575	1.074	1.158	0.0058	0.1481	0.0003	0.8336	0.1045	-20.3
SA501-9	0.1706	1.015	0.8122	0.0041	0.1498	0.0002	0.1044	0.1045	-0.17
SA501-10	0.1616	6.621	0.1174	0.0006	0.1110	0.0001	0.1044	0.1045	-0.14
SA564-2	0.1412	2.660	0.2556	0.0013	0.1186	0.0001	0.1043	0.1045	-0.25
SA564-3	0.0664	3.066	0.1042	0.0005	0.1102	0.0001	0.1044	0.1045	-0.13
KBA12-6	0.1620	4.345	0.1794	0.0009	0.1145	0.0001	0.1045	0.1045	-0.05
KBA12-8	0.1217	4.699	0.1246	0.0006	0.1114	0.0001	0.1044	0.1045	-0.11
Olivine Separate									
SA501-1OL	0.0184	8.552	0.0103	0.0002	0.1050	0.0001	0.1044	0.1045	-0.11

*SA501-7 was not used in calculations for age and initial ^{187}Os due to post-magmatic alteration.

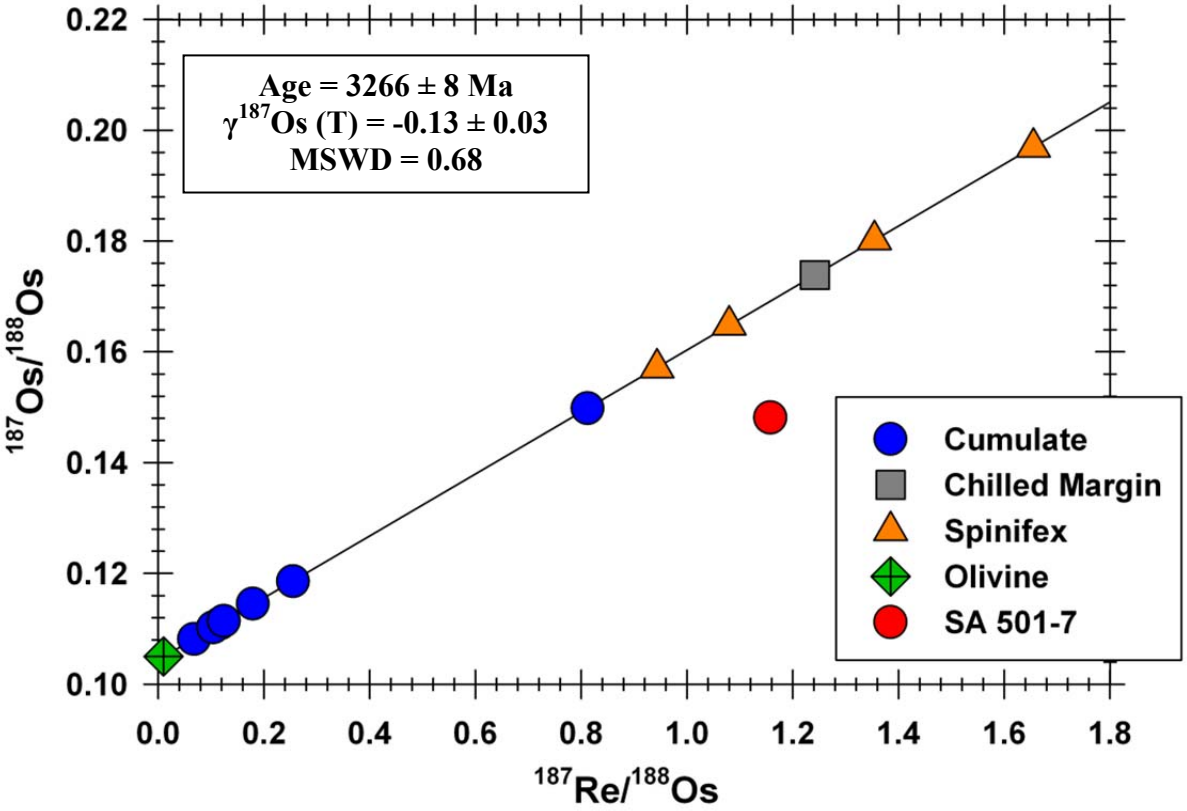

Figure 9. Re-Os isochron diagram for whole-rock komatiite samples and an olivine separate from the Weltevreden Formation. Sample SA-501-7, highlighted in red, was not included in calculations for age and γ^{187}Os. Error bars are smaller than the size of the symbols.

4.5 Major, minor, trace elements in the olivines

The average compositions of representative olivine grains are listed in Table VI. Approximately 80 olivine grains from six thin sections representing the three Weltevreden komatiite lava flows were analyzed. The olivines vary in MgO content from 49.9 – 52.5 wt.% MgO, and show the maximum of 95.1± 0.8 (flow SA501) forsterite content. These data are also similar to the data of Kareem and Byerly (2000). This confirms the notion that the olivines found in Weltevreden komatiites are among the most MgO-rich olivines ever found in terrestrial lavas. The most magnesian olivines chosen to be analyzed via LA-ICP-MS for more precise transition metal abundances are displayed in Table VII.

The average V content in the olivines from flow SA501 obtained via laser ablation ICP-MS analysis is 4.8 ± 0.3 ppm (N=24, $2\sigma_{mean}$). These data will be used to infer for the origin of the Weltevredn Fm.

Table VI.
Average major element compositions and *Fo* contents of olivines.

Sample	SiO_2	TiO_2	Al_2O_3	Cr_2O_3	FeO	MnO	NiO	MgO	CaO	%Fo
SA501-1 OL	41.2	0.001	0.001	0.214	4.90	0.071	0.427	52.5	0.162	95.0
SA501-8 OL	41.5	0.001	0.001	0.290	4.97	0.075	0.423	52.6	0.168	95.0
SA564-2 OL	40.7	0.001	0.001	0.276	7.82	0.116	0.379	50.1	0.173	91.9
SA564-3 OL	40.5	0.001	0.001	0.294	7.58	0.106	0.363	49.9	0.181	92.1
KBA12-6 OL	41.2	0.001	0.001	0.424	5.84	0.088	0.426	51.7	0.167	94.0
KBA12-8 OL	40.8	0.001	0.001	0.314	6.48	0.098	0.416	50.8	0.172	93.3

Table VII.
Average transition metals abundances (major: wt.%; minor: ppm) in the olivines and the chilled margin sample of the Weltevreden komatiites.

Sample	Sc	TiO_2	V	Cr	MnO	FeO	Co	Ni	Cu	Zn	Ga	Ge
SA564-6	27.3	0.186	124	2067	0.16	9.77	107	2067	14.5	77.2	5.3	1.3
SA501-1 Ol	2.14	0.002	4.71	1524	0.092	4.90	116	3519	2.07	39.3	0.167	0.902
SA501-8 Ol	2.99	0.003	4.97	1347	0.079	4.97	106	3327	2.17	31.9	0.175	0.813
BHVO-2G	479	0.10	376	351	0.0	0.10	353	388	427	403	372	433

V. Discussion and Implications

5.1 Origin of the Weltevreden source: wet or dry melts?

We use several lines of evidence to constrain the mode of origin for the Weltevreden komatiites magma.

(1) Water is highly incompatible during mantle melting, with the degree of incompatibility similar to that of Ce; the H_2O/Ce ratio is relatively constant in the modern upper mantle, and averages 207 ± 22, as compiled from the data of (Michael, 1995). The calculated Ce abundance in the Weltevreden source is 0.80 ± 0.05 ppm (Fig. 6), which translates into the H_2O content in the source of 166 ppm, or *ca*. 0.02 wt%, in the source. This indicates extremely dry conditions of the Weltevreden komatiite magma formation.

(2) Vanadium partitioning behavior in silicate magmas can be used as a redox indicator (Canil, 1997, 1999; Canil and Fedortchouk, 2001; Canil, 2002). It has been shown by these authors that during mafic magma differentiation, the major variable controlling $D_V^{ol/liq}$ is fO_2, with more oxidized, water-rich arc systems (higher fO_2) having $D_V^{ol/liq}$ <0.01, whereas in the less oxidized, essentially anhydrous, mantle plume and MORB-systems, $D_V^{ol/liq}$ ranges between 0.025 and 0.10. Using the calculated V content in the emplaced komatiite lava, and the average V content in the olivine, a precise $D_V^{ol/liq}$ value of 0.044±0.003 is obtained. This value is obtained by dividing the concentration of V in the solid phase (olivine: SA501-1OL) by the concentration of V content in the melt (chilled margin: SA564-6). The bulk differentiation D_V can be obtained from the regression of the V data for the whole-rock samples and the olivines. The regression analysis indicates a bulk differentiation solid-liquid D_V = 0.075±0.005. Both values are well within the range established for the anhydrous systems, and, together with the trace element argument presented above, are strong evidence for high-temperature, anhydrous origin of the Weltevreden komatiite magma.

5.2 Weltevreden komatiites and the temperatures in the Archean mantle

Taking into account that the Weltevreden magmas likely formed via anhydrous melting and by using the calculated emplaced lava composition and the protocol of Nisbet et al. (1993) and Abbott et al. (1994), we estimate a liquidus temperature of the emplaced komatiite lava to be 1600°C ± 10°C. This liquidus temperature, using the protocol of (McKenzie and Bickle, 1988; Abbott et al., 1994), is translated into the potential mantle temperature of 1830 ± 25°C, with the depths of melting initiation of ~530 km. This source was, thus, ~230°C hotter than the contemporary ambient mantle predicted by secular cooling models (*ca*. 1600°C: Richter, 1988). Such conditions, whereby the ascending material is >200°C hotter than the ambient mantle, are consistent with those projected for mantle plumes (e.g., Herzberg et al., 2007). Some thermal evolution models indicate mantle temperatures at *ca*. 3.3 Ga to range between 1500-1800°C (e.g., Korenaga, 2007; Labrosse and Jaupart, 2007; Herzberg et al., 2010), which our data suggest temperatures to be closer to the upper limit of these model estimates. Nevertheless, these data are, therefore, most consistent with a mantle plume origin for the Weltevreden komatiites.

VI. Concluding Remarks

(1). High-precision Re-Os isotopic and HSE abundance data obtained for a set of remarkably fresh komatiites from the Weltevreden Formation of the Barberton Greenstone Belt define an isochron with an age of 3266 ± 8 Ma and an initial $\gamma^{187}Os = -0.14 \pm 0.05$. The Weltevreden komatiite source is calculated to have contained absolute and relative HSE abundances similar to those in an average late Archean komatiite source of Puchtel et al. (2009b) and the total abundances that are 80% of those present in the modern PUM estimate of Becker et al. (2006). If the HSE budget of the terrestrial mantle has been established via accretion of large planetesimals after the last major interaction between the core and the mantle, our data indicate that by 3.3 Ga, these materials were largely homogenized within the mantle on the scale of mantle domains sampled by Weltevreden komatiites.

(2). The source of the Weltevreden komatiites was strongly depleted in highly incompatible lithophile trace elements and is calculated to have contained only *ca*. 0.02% H_2O. This piece of evidence together with the bulk differentiation solid-liquid $D_V = 0.044 \pm 0.003$ for the Weltevreden system indicate rather reduced conditions of the komatiite magma formation, similar to those present in modern plume systems.

(3). The Weltevreden komatiite lava contained *ca.* 31% MgO upon emplacement, is calculated to have had liquidus temperatures of *ca*. 1600°C, and represents one of the hottest and most magnesian lavas ever emplaced on the Earth's surface. The calculated potential mantle temperature of *ca*. 1830°C was *ca*. 230°C higher than that of the contemporary ambient mantle, which provide additional support to the plume origin model for the Weltevreden komatiites. Some models for thermal evolution indicate mantle temperatures at 3.3 Ga to range from 1600 to 1800°C (Korenaga, 2005). The calculated potential mantle temperatures indicate temperatures to be closer to the upper limit of these model estimates.

(4). The results of this study, when put into the context of geologic significance, testify to the power of technological advances in analytical techniques. The extremely small abundances of HSE require careful and precise geochemical analysis and measurement that has only recently been made possible. These data significantly enhance our understanding of early mantle evolution and can be applied to geochemical, geophysical, and tectonic models pertaining to the thermal evolution of early Earth. Improvements to these types of models can only further advance our understanding of early Earth processes and mechanics.

Acknowledgements

This work was made possible through the support by the NSF grant EAR-0946629 to Igor Puchtel; this support is gratefully acknowledged. A special thank you goes to my advisor, Dr. Igor Puchtel, who supported and mentored me throughout the research process. His teachings have provided me with the proper skills required to successfully reach my education and research goals. I would also like to thank Dr. Rich Walker, Dr. Phil Piccoli, Dr. Richard Ash, Dr. Ricardo Arevalo Jr., Masters Candidate Miriam Galenas, as well as my friends and family for their input and support.

References

Abbott, D.H., Burgess, L., Longhi, J., Smith, W.H.F., 1994. An empirical thermal history of the Earth's upper mantle. J. Geophys. Res. 99, 13835-13850.

Anhaeusser, C.R., 1985. Archean layered ultramafic complexes in the Barberton Mountain Land, South Africa, *in* Ayres, L.D., Thurston, P.C., Card, K.D., and Weber, W., eds., Evolution of Archean supracrustal sequences. Geological Association of Canada Special Paper 28.

Armstrong, R.A., Compston, W., DeWit, M.J., Williams, I.S., 1990. The stratigraphy of the 3.5-3.2 Ga Barberton greenstone belt revisited: A single zircon ion microprobe study. Earth and Planetary Science Letterrs 101 (1), 90-106.

Arevalo Jr., R. and McDonough, W.F., 2008. Tungsten geochemistry and implications for understanding the Earth's interior. Earth and Planetary Science Letters (272): 656-665, doi:10.1016/j.epsl.2008.05.031.

Arndt, N.T., Naldrett, A.J., and Pyke, D.R., 1977. Komatiitic and iron-rich tholeiitic lavas of Munro Township, northeast Ontario. Journal of Petrology, 18: 19-28.

Arndt, N.T., 1986. Differentiation of komatiite flows. Journal of Petrology 27 (2), 279-301.

Arndt, N.T., Ginibre, C., Chauvel, C., Albarède, F., Cheadle, M., Herzberg, C., Jenner, G., and Lahaye, Y., 1998. Were komatiites wet? Geology, 26 (8): 739-742.

Arndt, N.T., Lesher, C.M., Barnes, S.J., 2008. Komatiite. Cambridge, UK, Cambridge University Press.

Arndt, N.T., Lesher, C.M., Houle, M.G., Lewin, E., Lacaze, Y., 2004. Intrusion and crystallization of a spinifex-textured komatiite sill in Dundonald Township, Ontario. Journal of Petrology 45 (12): 2555-2571.

Arndt, N.T. and Nisbet, E.G., 1981. ***Komatiites.*** George Allen and Unwin, London, UK.

Barnes, S. J., Naldrett, A. J., and Gorton, M. P., 1985. The origin of fractionation of platinum group elements in terrestrial magmas. Chemical Geology, 53: 303-323.

Beattie, P., Ford, C., Russell, D., 1991. Partition coefficients for olivine-melt and orthopyroxene-melt systems. Contributions to Mineralogy and Petrology 109 (2), 212-224.

Becker, H., Horan, M.F., Walker, R.J., Gao, S., Lorand, J.-P., Rudnick, R.L., 2006. Highly siderophile element composition of the Earth's primitive upper mantle: Constraints from new data on peridotite massifs and xenoliths. Geochimica et Cosmochimica Acta 70 (17), 4528-4550.

Birck, J. L., Roy-Barman, M., and Capmas, F., 1997. Re-Os isotopic measurements at the femtomole level in natural samples. Geostandards Newsletter, 21: 19-27.

Brügmann, G.E., Arndt, N.T., Hofmann, A.W., Tobschall, H.J., 1987. Noble-metal abundances in komatiite suites from Alexo, Ontario, and Gorgona-Island, Columbia. Geochimica et Cosmochimica Acta 51 (8): 2159-2169.

Byerly, G.R., Kröner, A., Lowe, D.R., Todt, W., Walsh, M.M., 1996. Prolonged magmatism and time constraints for sediment deposition in the Early Archean Barberton greenstone belt - evidence from the Upper Onverwacht and Fig Tree Groups. Precambrian Research 78 (1-3), 125-138.

Canil, D., 1997. Vanadium partitioning and the oxidation state of Archaean komatiite magmas. Nature 389 (6653), 842-845.

Canil, D., 1999. Vanadium partitioning between orthopyroxene, spinel and silicate melt and the redox states of mantle source regions for primary magmas. Geochimica et Cosmochimica Acta 63 (3-4), 557-572.

Canil, D., Fedortchouk, Y., 2001. Olivine-liquid partitioning of vanadium and other trace elements, with applications to modern and ancient picrites. Canadian Mineralogist 39, 319-330.
Canil, D., 2002. Vanadium in peridotites, mantle redox and tectonic environments: Archean to present. Earth and Planetary Science Letters 195 (1-2), 75-90.
Chavagnac, V., 2004. A geochemical and Nd isotopic study of Barberton komatiites (South Africa): implication for the Archean mantle. Lithos 75 (3-4): 253-281.
Cohen, A. S. and Waters, F. G., 1996. Separation of osmium from geological materials by solvent extraction for analysis by thermal ionization mass spectrometry. Earth and Planetary Science Letters, 322: 269-275.
Creaser, R.A., Papanastassiou, D.A., Wasserburg, G.J., 1991. Negative Thermal Ion Mass-Spectrometry of Osmium, Rhenium, and Iridium. Geochimica et Cosmochimica Acta 55 (1), 397-401.
Crocket, J.H., Macrae, W.E., 1986. Platinum-group element distribution in komatiitic and tholeiitic volcanic-rocks from Munro township, Ontario. Econ. Geol. 81: 1242-1251.
Flanagan, F.J., 1976. Description and analyses of eight new USGS rock standards. USGS Professional Paper 840: 1-192.
Green, J. C., Nicholls, I. A., Viljoen, M. J., and Viljoen, R. P., 1974. Experimental demonstration of the existence of peridotitic liquids in earliest Archean magmatism. Geology, 3: 11-14.
Hamlyn, P.R., Keays, R.R., Cameron, W.E., Crawford, A.J., Waldron, H.M., 1985. Precious metals in magnesian low-Ti lavas - Implications for metallogenesis and sulfur saturation in primary magmas. Geochimica et Cosmochimica Acta 49 (8): 1797-1811.
Herzberg, C., Asimow, P.D., Arndt, N., Niu, Y.L., Lesher, C.M., Fitton, J.G., Cheadle, M.J., Saunders, A.D., 2007. Temperatures in ambient mantle and plumes: Constraints from basalts, picrites, and komatiites. Geochemistry Geophysics Geosystems 8, Article Q02006.
Herzberg, C., Condie, K., and Korenaga, J., 2010. Thermal history of the Earth and its petrological expression. Earth and Planetary Science Letters 292, 79-88.
Hofmann, A.W., 1988. Chemical differentiation of the Earth: The relationship between mantle, continental crust and oceanic crust. Earth and Planetary Science Letters 90 (3), 297-314.
Horan, M.F., Walker, R.J., Morgan, J.W., Grossman, J.N., Rubin, A.E., 2003. Highly siderophile elements in chondrites. Chemical Geology 196 (1-4), 5-20.
Huppert, H.E. and Sparks, R.S.J., 1985. Komatiites 1. Eruption and flow. Journal of Petrology 26 (3): 694-725.
Jochum, K.P., Willbold, M., Raczek, I., Stoll, B. and Herwig, K. 2005. Chemical characterization of the USGS reference glasses GSA-1G, GSC-1G, GSD- 1G, 175GSE-1G, BCR-2G, BHVO-2G and BIR-1G using EPMA, ID-TIMS, IDICP-MS and LA-ICP-MS. Geostd. Geoanalyt. Res. 29: 285-302.
Kareem, K. (2005). Komatiites of the Weltevreden Formation, Barberton Greenstone Belt, South Africa: Implications for the chemistry and temperature of the Archean mantle. Department of Geology and Geophysics. Baton Rouge, Louisiana State University. Doctor of Philosophy: 233.
Kareem, K.M., Byerly, G.R., 2003. Petrology and geochemistry of 3.3 Ga komatiites - Weltevreden Formation, Barberton Greenstone Belt. LPSC XXXIV, Houston, TX.
Keays,R.R., 1995. The role of komatiitic and picritic magmatism and S-saturation in the formation of ore-deposits. Lithos 34 (1-3): 1-18.

Korenaga, J., 2005. Archean geodynamics and the thermal evolution of Earth. Geophysical Monograph Series 164, 7-32.
Kröner, A., Hegner, E., Wendt, J.I., Byerly, G.R., 1996. The oldest part of the Barberton granitoid-greenstone terrain, South Africa: evidence for crust formation between 3.5 and 3.7 Ga. Precambrian Research 78 (1-3), 105-124.
Langmuir, C.H., Klein, E.M., and Plank, T., 1992. Petrological constraints on mid-ocean ridge basalts: constraints on melt generation beneath ocean ridges, Mantle flow and melt generation at mid-ocean ridges, Geophyscial Monograph 71: 183-280.
Labrosse, S. and Jaupart C., 2007. Thermal evolution of the Earth: Secular changes and fluctuations of plate characteristics. Earth and Planetary Science Letters 260, 465-481.
Lorand, J.P., Alard, O., Godard, M., 2009. Platinum-group element signature of the primitive mantle rejuvenated by melt-rock reactions: evidence from Sumail peridotites (Oman ophiolite). Terra NOVA 21 (1): 35-40.
Lowe, D.R., 1994. Accretionary history of the Archean Barberton Greenstone Belt (3.55-3.22 Ga), southern Africa. Geology 22 (12), 1099-1102.
Lowe, D.R., 1999. Geologic evolution of the Barberton Greenstone Belt and vicinity. In: R., L.D. and Byerly, G.R. (Ed.), Geological Evolution of the Barberton Greenstone Belt. Geological Society of America, Special Paper 329, Boulder, 287-312.
Lowe, D.R., Byerly, G.R., 1999. Stratigraphy of the west-central part of the Barberton Greenstone Belt, South Africa. In: R., L.D. and Byerly, G.R. (Ed.), Geological Evolution of the Barberton Greenstone Belt. Geological Society of America, Special Paper 329, Boulder, 1-36.
Lowe, D.R., Byerly, G.R., 2007. An overview of the geology of the Barberton Greenstone Belt and vicinity: Implications for early crustal development. In: Van Kranendonk, M.J., Smithies, R.H., and Bennett, V.C. (Ed.), Earth's Oldest Rocks. Elsevier, Amsterdam, 15, 481-526.
Ludwig, K.R., 2003, ISOPLOT/Ex, A geochronological toolkit for Microsoft Excel: Berkeley Geochronology Center Special Publication 4: 1-70.
Mavrogenes, J.A. and O'Neill, H.S.C., 1999. The relative effects of pressure, temperature and oxygen fugacity on the solubility of sulfide in mafic magmas. Geochimica et Cosmochimica Acta 63 (7-8): 1173-1180.
McDonough W. F. and Sun S. S. 1995. The composition of the Earth. Chemical Geology 120(3-4), 223-253.
McKenzie, D., Bickle, M.J., 1988. The volume and composition of melt generated by extension of the lithosphere. Journal of Petrology 29 (3), 625-679.
Mertzman, S.A., 2000. K-Ar results from the southern Oregon - northern California Cascade range. Oregon Geology 62 (4), 99-122.
Michael, P., 1995. Regionally Distinctive Sources of Depleted MORB - Evidence from Trace-Elements and H_2O. Earth and Planetary Science Letters 131 (3-4), 301-320.
Morgan, J.W., Wandless, G.A., Petrie, R.K., and Irving, A.J., 1981. Composition of the Earth's upper mantle - 1. Siderophile trace elements in ultramafic nodules. Tectonophyics 75: 47-67.
Morgan J.W., 1985. Osmium isotope constraints on Earth’s late accretionary history. Nature 317: 703–705.
Morgan J.W., 1986. Ultramafic xenoliths: Clues to Earth’s late accretionary history. J. Geophys. Res. 91: 12375–12387.

Nesbitt, R.W., Sun, S.S., 1976. Geochemistry of Archaean spinifex-textured peridotites and magnesian and low-magnesian tholeiites. Earth and Planetary Science Letters 31 (3), 433-453.

Nisbet, E. G., Arndt, N. T., Bickle, M. J., Cameron, W. E., Chauvel, C., Cheadle, M., Hegner, E., Kyser, T. K., Martin, A., Renner, R., and Roedder, E., 1987. Uniquely fresh 2.7 Ga komatiites from the Belingwe Greenstone Belt, Zimbabwe. Geology 15: 1147-1150.

Nisbet, E.G., Cheadle, M.J., Arndt, N.T., Bickle, M.J., 1993. Constraining the potential temperature of the Archaean mantle: A review of the evidence from komatiites. Lithos 30 (3-4), 291-307.

Norman, M.D., Griffin, W.L., Pearson, N.J., Garcia, M.O. and O'Reilly, S.Y., 1998. Quantitative analysis of trace element abundances in glasses and minerals: a comparison of laser ablation inductively coupled plasma mass spectrometry, solution inductively coupled plasma mass spectrometry, proton microprobe and electron microprobe data. Journal of Analytical Atomic Spectrometry 13: 477-482.

Parman, S. W., Grove, T. L., and Dann, J. C., 2001. The production of Barberton komatiites in an Archean subduction zone. Geophysical Research Letters, 28 (13): 2513-2516.

Pearce, N.J.G., Perkins, W.T., Westgate, J.A., Gorton, M.P., Jackson, S.E., Neal, C.R. and Chenery, S.P. 1997. Compilation of new and published major and trace element data for NIST SRM 610 and NIST SRM 612 glass reference materials. Geostd. News. 21, 115-144.Puchtel, I.S., Hofmann, A.W., Mezger, K., Shchipansky, A.A., Kulikov, V.S., Kulikova, V.V., 1996. Petrology of a 2.41 Ga remarkably fresh komatiitic basalt lava lake in Lion Hills, central Vetreny Belt, Baltic Shield. Contrib. Mineral. Petrol. 124, 273-290.

Puchtel, I.S., Humayun, M., 2001. Platinum group element fractionation in a komatiitic basalt lava lake. Geochimica et Cosmochimica Acta 17 (65), 2979-2993.

Puchtel, I.S., Brandon, A.D., Humayun, M., 2004a. Precise Pt-Re-Os isotope systematics of the mantle from 2.7-Ga komatiites. Earth and Planetary Science Letters 224 (1-2), 157-174.

Puchtel, I.S., Humayun, M., Campbell, A., Sproule, R., Lesher, C.M., 2004b. Platinum group element geochemistry of komatiites from the Alexo and Pyke Hill areas, Ontario, Canada. Geochimica et Cosmochimica Acta 68 (6), 1361-1383.

Puchtel, I.S., Humayun, M., 2005. Highly siderophile element geochemistry of ^{187}Os-enriched 2.8-Ga Kostomuksha komatiites, Baltic Shield. Geochimica et Cosmochimica Acta 69 (6), 1607-1618.

Puchtel, I.S., Humayun, M., Walker, R.J., 2007. Os-Pb-Nd isotope and highly siderophile and lithophile trace element systematics of komatiitic rocks from the Volotsk suite, SE Baltic Shield. Precambrian Research 158 (1-2), 119-137.

Puchtel, I.S., Walker, R.J., Anhaeusser, C.R., Gruau, G., 2009a. Re-Os isotope systematics and HSE abundances of the 3.5 Ga Schapenburg komatiites, South Africa: Hydrous melting or prolonged survival of primordial heterogeneities in the mantle? Chemical Geology 262 (3-4), 391-405.

Puchtel, I.S., Walker, R.J., Brandon, A.D., Nisbet, E.G., 2009b. Pt-Re-Os and Sm-Nd isotope and HSE and REE systematics of the 2.7 Ga Belingwe and Abitibi komatiites. Geochimica et Cosmochimica Acta 73 (20), 6367-6389.

Rehkamper, M., Halliday, A.N., Fitton, J.G., Lee, D.-C., Wieneke, M., Arndt, N.T. 1999. Ir, Ru, Pt and Pd in basalts and komatiites: New constraints for the geochemical behavior of the platinum group elements in the mantle. Geochim. Cosmochim. Acta. 63: 3915-3934.

Righter, K., 2003. Metal-silicate partitioning of siderophile elements and coreformation in early Earth. Annual Review of Earth and Planetary Sciences 31: 135-174.
Richter, F.M., 1988. A major change in the thermal state of the Earth at the Archean-Proterozoic boundary: Consequences for the nature and preservation of continental lithosphere. Journal of Petrology Spec. Lithosphere Issue, 39-52.
Robin, C., Arndt, N., Chauvel, C., Byerly, G., Kareem, K., Hofmann, A., Wilson, A., 2009. 300 m.y. of komatiit evolution in the Barberton Greenstone Belt. Geochimica et Cosmochimica Acta 73 (13): A1108.
Roeder, P.L., Emslie, R.F., 1970. Olivine-liquid equilibrium. Contributions to Mineralogy and Petrology 29 (4), 275-282.
Shirey, S.B., 1997. Re-Os isotopic compositions of midcontinent rift system picrites: Implications for plume-lithosphere interaction and enriched mantle sources. Canadian Journal of Earth Sciences 34 (4): 489-503.
Shirey, S.B., Walker, R.J., 1998. The Re-Os isotope system in cosmochemistry and high-temperature geochemistry. Annual Reviews of Earth and Planetary Sciences 26, 423-500.
Smith, H.S., Erlank A.J., Duncan, A.R., 1980. Geochemistry of some ultramafic komatiite lava flows from the Barberton Mountain Land South Africa. Precambrian Research 11 (3-4): 399-415.
Smoliar, M.I., Walker, R.J., Morgan, J.W., 1996. Re-Os ages of Group IIA, IIIA, IVA, and IVB iron meteorites. Science 271 (5762), 1099-1102.
Stiegler M. T., Lowe, D. R., and Byerly, G. R., 2008. Abundanct pyroclastic komatiitic volcanism in the 3.5 – 3.2 Ga Barberton greenstone belt, South Africa. Geology, 36 (10): 779-782; doi: 10.1130/G24854A.1.
Sun, S. S. and Nesbitt, R. W., 1978. Petrogenesis of Archean ultrabasic and basic volcanics: evidence from rare earth elements. Contributions to Mineral Petrology, 65: 301-325.
Thompson, M.E., Kareem, K.M., Xie, X., Byerly, G.R., 2003. Fresh melt inclusions in 3.3 Ga komatiitic olivines from the Barberton Greenstone Belt, South Africa. LPSC XXXIV, Houston, TX.
Viljoen, M.J., Viljoen, R.P., 1969a. The geology and geochemistry of the Lower Ultramafic Unit of the Onverwacht Group and a proposed new class of igneous rock. Geological Society of South Africa Special Publication 2, 55-86.
Viljoen, M.J., Viljoen, R.P., 1969b. Evidence for the existence of a mobile extrusive peridotitic magma from the Komati formation of the Onverwacht Group. Geological Society of South Africa Special Publication 2, 87-112.
Viljoen, M.J., Viljoen, R.P., Smith, H.S., Erlank, A.J., 1983. Geological, textural and geochemical features of komatiitic flows from the Komati Formation. Geol. Soc. South Africa Spec. Publ. 9, 1-20.
Walker, D., 2000. Core partitioning in mantle geochemistry: Geochimical Society Ingerson Lecture, GSA Denver, October 1999. Geochimica et Cosmochimica Acta 64 (17): 2897-2911.
Walker, R.J., Shirey, S.B., Stecher, O., 1988. Comparitive Re-Os, Sm-Nd and Rb-Sr isotope and trace element systematics for Archean komatiite flows from Munro Township, Abitibi Belt, Ontarios. Earth Planetary Science Letters 87: 1-12.
Walker, R.J., Carlosn, R.W., Shirey, S.B., and Boyd, F.R., 1989. Os, Sr, Nd, and Pb isotope systematics of southern African peridotite xenoliths: Implications for the chemical evolution of subcontinental mantle. Geochimica et Cosmochimica Acta 53: 1583-1595.

Walker, R.J., Echeverría, L.M., Shirey, S.B., and Horan, M.F., 1991. Re-Os isotopic constraints on the origin of volcanic rocks, Gorgona Island, Columbia: Os isotopic evidence for ancient heterogeneities in the mantle. Contributions to Mineral Petrology 107: 150-162.

Walker, R.J., Storey, M., Kerr, A., Tarney, J., and Ardnt, N.T., 1999. Implications of ^{187}Os heterogeneities in mantle plumes: evidence from Gorgona Island and Curaçao. Geochimica et Cosmochimica Acta 63: 907-910.

Walker, R.J., 2009. Highly siderophile elements in the Earth, Moon and Mars: Update and implications for planetary accretion and differentiation. Chemie der Erde - Geochemistry 69 (2), 101-125.

Wilson, A.H., Shirey, S.B., Carlson, R.W., 2003. Archean ultra-depleted komatiites formed by hydrous melting of cratonic mantle. Nature 423 (6942): 858-861.

Appendix

Honor Code

I pledge on my honor that I have not given or received any unauthorized assistance or plagiarized on this assignment.

_____

Brian Daniel Connolly